Antimicrobial Effect of Silver-Embedded Titania Nanotube Implant Surface Against *Porphyromonas Gingivalis*

BY

AMY SHYUAN AU
B.A.A.S., University of Pacific, 2012
D.D.S., University of Pacific Arthur A. Dugoni School of Dentistry, 2012
Prosthodontics Candidate, University of Illinois at Chicago, 2015

THESIS

Submitted as partial fulfillment of the requirements
for the Degree of Master of Science in Oral Sciences
in the Graduate College of the
University of Illinois at Chicago, 2015

Chicago, Illinois

Defense Committee:
Dr. Cortino Sukotjo, Chair and Advisor
Dr. Tolou Shokuhfar, Michigan Technological University
Dr. Christine D. Wu, Pediatric Dentistry
Dr. Stephen D. Campbell, Restorative Dentistry
Dr. Kent L. Knoernschild, Restorative Dentistry

This is dedicated to my dear family in California and the new family I found while in Chicago. Their constant support allows me to follow my passion.

ACKNOWLEDGEMENTS

I would like to thank my thesis committee – Dr.'s Cortino Sukotjo, Tolou Shokuhfar, Christine Wu, Stephen Campbell, and Kent Knoernschild—for their support and assistance. They provided guidance that helped me accomplish my research project. I would also like to thank Sweetu Patel and Dr. Wei Li, both of whom provided tremendous help with the technical aspects of the research, without which this project would not be possible.

This project was also made possible by the following grants: 2013 IADR Prosthodontics Group Student Research Fellowship, 2013 Greater New York Academy of Prosthodontics Student Grant, 2013 Academy of Prosthodontics Student Award Grant, 2013 ACPEF Research Grant, and National Science Foundation DMR Award No. 1307052.

TABLE OF CONTENTS

CHAPTER PAGE

I. INTRODUCTION……1
1.1 Background……1
1.2 Statement of the Problem……1
1.3 Purpose of the Study……2
1.4 Significance of the Problem……2
1.5 Significance of the Study……2
1.6 Specific Aims and Hypotheses ……3

2 CONCEPTUAL FRAMEWORK AND RELATED LITERATURE……5
2.1 Early Dental Implants and Osseointegration ……5
2.2 Titanium Dental Implants & Implant Surface Modification……7
2.2.1 Current Dental Implant Surface Modifications……9
2.3 Nanotechnology, Nanomedicine, and Nanotubes ……11
2.4 Titanium Nanotubes via Anodization ……13
2.4.1 Antimicrobial Potential of Nanotubes……14
2.4.2 Biocompatibility of Nanotubes……16
2.5 Peri-implantitis and Peri-mucositis ……18
2.5.1 Diagnosis of Peri-implantitis ……18
2.5.2 Treatment of Peri-implantitis ……20
2.6 *Porphyromonas gingivalis* ……23
2.6.1 *P. gingivalis* vs. Titanium ……23
2.7 Silver & Implant Dentistry ……26
2.7.1 *In vitro* studies on Nanotubular Titanium ……27
2.7.2 Silver's Mechanism of Action ……29

3 METHODS……31
3.1 Preparation of Samples……31
3.1.1 Anodization……32
3.2 Surface Characterizations……35
3.2.1 Fourier Transform Infrared Spectroscopy (FTIRS) ……35
3.2.2 Field Emission Scanning Electron Microscopy (FESEM) & Energy Dispersive X-ray Spectroscopy (EDX) ……35
3.2.3 Water Contact Angle (WCA) ……36
3.2.4 White Light Interferometry (WLI) ……36
3.3 *Porphyromonas gingivalis* Biofilm Attachment ……37
3.3.1 *In Vitro* Attachment Assay ……37
3.3.2 Live/Dead Stain ……38
3.3.3 FESEM……39
3.3.4 Statistical Analysis ……40

4 RESULTS……41
4.1 Surface Characterizations ……41
4.1.1 FTIR……41

TABLE OF CONTENTS (continued)

CHAPTER PAGE

4.1.2 FESEM & EDX ……42
4.1.3 WCA ……44
4.1.4 WLI……46
4.2 Bacterial Attachment ……48
4.2.1 *In vitro* Attachment Assay ……48
4.2.2 Live/Dead Staining ……56
4.2.3 FESEM ……58

5 DISCUSSION……61
5.1 Summary……61
5.2 Characterizations……62
5.2.1 FTIR……62
5.2.2 FESEM & EDX ……63
5.2.3 WCA & Wettability ……63
5.2.4 WLI……65
5.3 *P. gingivalis* Biofilm Attachment ……67
5.3.1 *In vitro* Attachment Assay ……67
5.3.2 Live/Dead Stain……69
5.3.3 FESEM ……69
5.3.4 Summary of *P. gingivalis* Biofilm Attachment……70
5.4 Integration of All Results……73
5.5 Weaknesses and Limitations of this Study ……77
5.6 Clinical Relevance……82

6 CONCLUSIONS……84
6.1 Summary……84
6.2 Recommendations for Future Work……87

7 CITED LITERATURE……90

8 APPENDIX……96
8.1 VITA……96

LIST OF TABLES

TABLE PAGE

1. Water Contact Angle Readings for all Groups over 26 days……44
2. White light interferometry readings for surface roughness ……45
3. Preliminary Data: Initial OD_{550} readings for *P. gingivalis* attachment to CP-Ti. ……48
4. Initial OD_{550} readings of extracted crystal violet stain for *P. gingivalis* attachment to titania surfaces. (EXPT #1) ……49
5. Individual surface sample dimension measurements (mm) and calculated surface area (mm^2). (EXPT #1) ……50
6. *P. gingivalis* attachment based on spectrophotometer reading of extracted crystal violet stain from titania surfaces OD_{550} per mm^2 (EXPT #1) ……51
7. Initial OD_{550} readings of extracted crystal violet stain for *P. gingivalis* attachment to titania surfaces. (EXPT #2) ……53
8. Individual surface sample dimension measurements (mm) and calculated surface area (mm^2). (EXPT #2) ……54
9. *P. gingivalis* attachment based on spectrophotometer reading of extracted crystal violet stain from titania surfaces OD_{550} per mm^2 (EXPT #2) ……55
10. Comprehensive Summary of All Results……73

LIST OF FIGURES (including illustrations)

FIGURE PAGE

1. FESEM and EDX from previous anodization protocol ……14
2. Diagram of the Workflow of the Project ……31
3. Diagram of the Anodization Technique……32
4. Fourier transform infrared spectroscopy analysis ……41
5. Field emission scanning electron microscopy and Energy-dispersive X-ray spectroscopy Results ……43
6. Water Contact Angle for all six different titanium surfaces ……45
7. White light interferometry readings for surface roughness……46
8. CP-Ti, TiNT, TiNT-Ag surfaces with attached *P. gingivalis* after crystal violet stain ……52
9. Graph of *P. gingivalis* attachment on various titanium surfaces (EXPT #1) ……52
10. Graph of *P. gingivalis* attachment on various titanium surfaces (EXPT:#2) ……55
11. *P. gingivalis* viability: Live/Dead Stain……56
12. FESEM images for the surfaces after bacterial inoculation and incubation. ……..58-60

LIST OF ABBREVIATIONS OR NOMENCLATURE

Ag	Silver
ANOVA	Analysis of Variance
CFU	Colony forming unit
CP-Ti	Commercially Pure Titanium
DI-water	Deionized water
EDX	Energy-dispersive X-ray spectroscopy
EtOH	Ethanol
EXPT	Experiment
FESEM	Field emission scanning electron microscopy
FTIR	Fourier transform infrared spectroscopy
HA	Hydroxyapatite
keV	kiloelectron volt
MBC	Minimum bactericidal concentration
MIC	Minimum inhibitory concentration
MTS	3-(4,5-dimethylthiazol-2-yl)-5-(3-carboxymethoxyphenyl)-2-(4-sulfophenyl)-2H-tetrazolium,inner salt
OD_{nm}	Optical Density/ Spectrophotometer reading
PCR	Polymerase chain reaction
PES	Phenazine ethosulfate
PBS	Phosphate buffer solution
SD	Standard Deviation
THB	Tod-Hewitt broth

TiNT	Titania Nantobular Surface with no silver
TiNT-Ag-0	Titania Nanotubular surface with silver intentional deposition of 0 second
TiNT-Ag-5	Titania Nanotubular surface with silver intentional deposition of 5 seconds
TiNT-Ag-10	Titania Nanotubular surface with silver intentional deposition of 10 seconds
TiNT-Ag-30	Titania Nanotubular surface with silver intentional deposition of 30 seconds
WCA	Water Contact Angle
WLI	White Light Interferometery

SUMMARY

Objectives: To fabricate and characterize silver and non-silver embedded titania nanotubes surfaces (TiNT-Ag and TiNT) and to investigate their effect on *Porphyromonas gingivalis* biofilm attachment.

Methods: TiNT and TiNT-Ag (0, 5 10, and 30 seconds reverse polarity) surfaces were fabricated on commercially pure Ti (CP-Ti) sheet by using a two step anodization procedure in an electrolyte composed of 80 % 1,2-propane diol and 20% deionized water (v/v) with or without AgF (0.66%, w/v). For surface characterization, the analyses utilized were fourier transform infrared (FTIR) spectroscopy, energy-dispersive X-ray (EDX) spectroscopy, field emission scanning electron microscopy (FESEM), white light interferometry (WLI), and water contact angle (WCA) analysis. For biofilm attachment, TiNT and TiNT-Ag surfaces were inoculated with *P. gingivalis* 33277 and incubated anaerobically at 37°C. After 12 hr, samples were stained with crystal violet and biofilm attachment was determined based on the amount of dye absorption (OD_{550nm}). All assays were performed independently 3 times in triplicate. Data were analyzed by one-way ANOVA and Tukey's HSD test ($\alpha = 0.05$).

Results: FTIR analysis showed characteristic absorption peaks at 2200 - 2800 cm^{-1} for Ag^{+} and Ti^{+} interaction with CO_2 and 500-1100 cm^{-1} for Ti-O and Ag-O bond stretch. FESEM revealed uniform titania nanotubes on surfaces with diameters ranging 80 – 100 nm. EDX spectra showed the presence of silver along with other known elements including

titanium, oxygen, carbon and fluoride. The R_a and WCA at Day 0 of the CP-Ti, TiNT, TiNT-Ag-0, TiNT-Ag-5, TiNT-Ag-10, and TiNT-Ag-30 were 0.10±0.01 μm, 9.84±0.25 μm, 0.31±0.02 μm, 0.30±0.02 μm, 0.29±0.02 μm, and 0.37±0.03 μm, and 7.4 ± 2.4°, 8.05 ± 2.2°, 8.95 ± 4.7°, and 6.25°± 1.518°, respectively. Statistically significant reduction (>87%) in *P. gingivalis* attachment was noted on all TiNT-Ag surfaces compared with the non-silver embedded TiNT surfaces ($P<0.05$). No significant differences in bacterial attachment were detected among the various TiNT-Ag groups. FESEM and live/dead stain of the inoculated surfaces confirmed the presence of bacteria on the surfaces and reduction of bacterial attachment on the silver surfaces.

Conclusions: Silver-embedded titania nanotubes were successfully fabricated on Ti surface by using the two step anodization procedure. Titanium nanotubular surfaces have increased surface wettability and surface roughness compared to commercially pure titanium surfaces. The incorporation of silver into the surfaces resulted in a more clinically desirable dental implant surface in terms of surface wettability, surface roughness, and uniform surface morphology. The surface architecture and characteristics of TiNT and TiNT-Ag were stable over 26 days. The titania nanotubular surface may have potential for improved bone response and ongoing tissue health. These surfaces suppressed the *in vitro* formation and attachment of *P. gingivalis* biofilm. The antimicrobial properties of silver-embedded titania nanotubes surfaces may contribute to the reduction of bacterial colonization, reduced inflammation, reduced clinical peri-implant complication, and improved ongoing hard and soft tissue peri-implant health.

1. INTRODUCTION

1.1 Background

The endosteal dental implants that are commonly used for dental patients have become one of the standard, reliable treatment options for tooth replacement.[1] Dental implants have shown great success rates of 96.5% and reported an increase in patient satisfaction and quality of life.[2, 3]

1.2 Statement of the Problem

Even after a dental implant becomes osseointegrated, it can be expected to have yearly bone loss and possible biologic and prosthetic complications.[2, 4, 5] This is a concern that current researchers of dental implant surfaces are trying to address by changing the surface features of the dental implant to not only improve osseointegration, but also possibly reduce the bone loss around the implants over time.[6] In a narrative and systematic review by Qian *et al.* 2012, marginal bone loss around dental implants was found in some insistences to occur as a natural, non-pathologic response that may be related to "combined factors" such as "implant hardware, clinical handling, and patient characteristics." The exposed threads became a new surface for potential food and plaque accumulation that could induce secondary peri-implant conditions.[7] Furthermore, if the peri-implant conditions such as peri-mucositis and peri-implantitis did occur, no standard of care has been established for the treatment of these conditions.[8] Even with the most careful surgical technique and a disinfected site, bacteria could adhere to the suture material and traverse through the patient's tissue, presenting an early bacterial challenge.[9]

1.3 Purpose of the Study

The purpose of this study was to create a novel silver-embedded titania nanotubular (TiO_2-NT-Ag or TiNT-Ag) dental implant surface and to investigate *Porphyromonas gingivalis* bacterial attachment onto TiNT-Ag surfaces containing different quantities of silver. We attempted to optimize an effective *in vitro* silver concentration for *P. gingivalis* growth inhibition. The novel dental implant surface may also improve osseointegration of titanium dental implants and reduce any bacterial associated peri-implant conditions.[6, 10]

1.4 Significance of the Problem

Over the past few decades, practitioners and researchers have observed improved osseointegration when surface modifications were included at both the macro and micro level. The faster the osseointegration of a dental implant, the less healing time required for patients, which may improve their quality of life. However, implant related complications are still prominent and difficult to treat, often requiring implant removal and revision surgery.[11, 12] The treatment of peri-implant conditions have shown to be tricky, unpredictable, and seem doomed once bacterial biofilm has formed on the dental implant.[8] Recent research on nanoscale dental implant surface modifications shows potential for improved osseointegration.

1.5 Significance of the Study

Our titania nanotubular surface embedded with silver would be a novel, dynamic dental implant surface that would not only improve osseointegration based on its nanofeatures, but also maintain marginal bone levels long-term compared to existing commercial dental

implant surfaces over time. The embedded silver may induce a host response modulation that could prevent biofilm formation and simplify necessary treatment, if any, of initial and future bacterial mediated peri-mucositis and peri-implantitis conditions for the patient.[10]

1.6 Specific Aims & Hypotheses

Aim #1: To fabricate silver deposited and non-silver deposited titania nanotubes using electrochemical anodization technique. A literature review of surface modifications for titanium dental implants was completed, and titanium nanotubes with silver seems promising as a novel, dynamic, biomimetic surface that can be fabricated. No research exists on the silver embedment in titanium nanotubes via anodization. **Hypothesis #1: Using previously established techniques, titania nanotubular surfaces with and without silver can be predictably fabricated to preset dimensions.**

Aim #2: To characterize the silver deposited and non-deposited titania nanotubes using water contact angle analysis, fourier transform infrared spectroscopy, energy-dispersive X-ray spectroscopy, and field emission scanning electron microscopy. After each surface type was fabricated, a portion of the samples was used solely for surface characterizations and analysis to determine the surface profile. **Hypothesis #2: The silver deposited and non-deposited titania nanotubular surfaces can be successfully characterized in many ways to show consistent and uncontaminated surface qualities.**

Aim #3: To investigate the antibacterial effect of silver embedded titania nanotube (TiNT-Ag) against the periodontal pathogen, *Porphyromonas gingivalis.* *P. gingivalis* was cultured and plated on both the silver and non-silver embedded nanotubular surfaces to determine the antimicrobial potential of each kind of surface. **Hypothesis #3: The novel nanotubular titania surfaces embedded with silver possess antimicrobial activity against *P. gingivalis*.**

Aim #4: To optimize an effective *in vitro* silver concentration for *Porphyromonas gingivalis* growth inhibition. Silver was deposited at various time intervals into the titanium nanotubes to see if the minimum inhibitory amount of silver as an antimicrobial agent could be discovered. **Hypothesis #4: An effective *in vitro* amount of silver will be found for *P. gingivalis* growth inhibition.**

2 CONCEPTUAL FRAMEWORK AND RELATED LITERATURE

2.1 Early Dental Implants & Osseointegration

Early dental implants of the 20th century include subperiosteal, transosteal, and endosteal implants. In 1977, Per-Ingvar Branemark presented his data of endosteal implants with successful osseointegration over a 10-year follow up. [13] This was auspicious as a new treatment modality for the partially and fully edentulous patients and opened the door to numerous kinds of restorative treatment options.

"Osseointegration" was first defined as a direct bone-to-implant interface by Branemark.[14] This was visible at a light microscope level. There was a structural and functional connection between the fixture and the load-bearing bone. According to the current Glossary of Prosthodontic Terms, osseointegration is defined as the "the apparent direct attachment or connection of osseous tissue to an inert, alloplastic material without intervening connective tissue."[15] In reality under the SEM, there is about 60-90% bone-to-implant contact, and there is a zone of up to 200A of proteoglycans between the bone and implant.[16] Osseointegration occurs over four stages: hemostasis, inflammatory, proliferative, and remodeling.[17, 18]

When an implant is first placed, the mechanical friction holding it in place is termed primary implant stability.[17, 18] Osseointegration can be described as the complex sequence of healing and bone remodeling that follows to provide long-term implant stability. Hemostasis occurs within minutes of implant placement, as platelets and fibrin form a blood clot around the surgical site. The inflammatory phase is next where immune cells are summoned from the blood stream via bradykinins, and they attempt to remove foreign

agents and bacteria alike. Macrophages assist with bacteria clearance via phagocytosis too. On day 3 or 4, the proliferative phase begins where fibroblasts arrive and generate the extracelluluar matrix. The mesenchymal cells then come in and start creating new blood vessels and activating osteoclasts via osteoinduction. Osteoinduction is defined as the recruitment of undifferentiated pluripotent cells and stimulating them to become preosteoblasts. Osteogenesis follows. [17, 18] Osteoconduction is when bone grows on a surface and is a quality inherent to all successful dental implant materials. Eventually, the first woven bone is formed on the implant that takes up to a week and concludes the proliferative stage. The final remodeling stage begins when bone commences remodeling to become trabecular in form. Osteoblasts start surrounding themselves with lamellar bone. The remodeling stage takes up to 3-4 months to complete. Current research looks to accelerate the stages of osseointegration for earlier clinical use of dental implants for patient satisfaction.

As previously described, the first dental implants were turned or machined.[14] Multiple implant success criteria were formulated by multiple groups. Albrektsson *et al.* noted that there needed to be no mobility of the implant, no peri-implant radiolucency, vertical bone loss ≤0.2mm after the 2nd year, no persistent pain, no infection, neuropathy, nor paresthesia.[4] By his criteria, there was a noted success rate of 85% after 5 years, and 80% after 10 years.[4] At present, implant survival rates are now reportedly much higher than in 1986. For full mouth rehabilitation on implants, survival rate can be as high as 97.2% in flapless computer-guided surgeries.[3]

2.2 Titanium Dental Implants & Implant Surface Modifications

Dental implants, like many other dental materials, are selected based on their cost, biocompatibility, ease of use, minimal bone trauma, and high survival rate.[19] Implant materials that are utilized include porcelain, stainless steel, cobalt chrome, titanium, and titanium alloys.[20] Due to high biocompatibility, low cost, high corrosion resistance, and desirable mechanical properties, commercially pure titanium has become the standard dental implant material.[17, 21] Titanium also has select use in dentistry for PFM restorations and removable prosthetics. The biocompatibility and corrosion resistance of titanium is attributed to the stable oxide film that forms at a thickness of <1nm.

In a study by Velten's group, titanium when exposed to air readily reacted with oxygen to form oxides up to 10nm thick at room temperature.[22] As they performed thermal oxidation of titanium with increased temperature, a thicker oxide layer could be formed as well, and an increased corrosion resistance was observed when the diameter of the nanotubes was about 100nm.[22] The experiment also showed that with anodic oxidation, the growth of the thickness of the titanium oxide layer could be more predictably controlled in a linear fashion.[22] The thermal oxidation method exhibited a more logarithmic pattern of growth of oxide layer. The oxide layer not only increased corrosion resistance but also was osteoconductive.

Surface hydrophilicity of a dental implant has been shown to be affected by surface free energy and surface roughness. Surface free energy varies depending on the element composition. The higher the surface free energy of an element, the more likely water will

bond to it and the higher the element's affinity for adsorption. Therefore, an increase of that particular element on a surface will lead to an increase of water attachment to that portion of the surface.[23, 24] Water contact angle is also affected by surface roughness and morphology, which in the case of nanotubes, can have capillary action of water into the nanotubes. If the surface roughness becomes too high, then the water may avoid it and air may be trapped instead.[25] In a study by Mekayarajjananoth *et al.*, the results showed a correlation between an increase of surface roughness of titanium dental implants and the increase of water contact angles, which decreased the overall wettability of the surface.[26]

Albrektsson and Wennerberg also classified the various surface roughness (R_a) of dental implants.[27] Smooth implants had R_a = 0-0.4μm and were found to be the smoothness of abutments and certain machined implants. This category was too smooth for proper osseointegration. Minimally rough surfaces had R_a = 0.5-1.0 μm, and many (turned) implants manufactured prior to 1995 displayed this roughness. There was the longest clinical documentation for this category. Moderately rough implants had R_a = 1.0-2.0 μm and describe most currently used implants, including Osseospeed, SLA, and TiUnite. This group had an observed stronger bone response and better clinical success than turned implants, although long-term documentation was lacking. Rough surface implants had R_a > 2.0 μm such as the plasma-sprayed titanium and hydroxyapapite coated implants that had up to 5 year follow-up. There was an increased incidence of peri-implantitis reported in some studies for the rough surface implants. Although the moderately rough group seemed to perform better than the other groups, the difference in performance among the minimally rough, moderately rough, and rough surfaces was not statistically significant.

2.2.1 Current Dental Implant Surface Modifications

Surface modifications of dental implants have been extensively researched in an attempt to improve dental implant performance. Jokstad *et al.* completed a systematic review of all currently used dental implants present to determine which types had better clinical performances.[28] Over the 220 brands of implants, only 10 provided extensive clinical evidence of use. Surface modifications included acid etching, blasted surface, hydroxyapapite (HA) coating, oxidized surface, titanium plasma spray, and turned surfaces, as embodied by the 3i Osseotite®, Astra TiOblast®, Straumann SLA®, Lifecore Sustain®, Nobel TiUnite®, Straumann ITI® TPS, and Nobel Branemark System ®ML III implants, respectively. The sandblasted surfaces employed aluminous oxide particles in fabrication. The acid etch utilized either hydrogen chloride or sulfate. Almost all of the resulting surfaces created a rough, isotropic surface. The etched surfaces performed better than the turned surfaces (95% vs. 87%). The SLA and TPS surfaces performed equally well. The reviewers also noted that the clinical success was affected by factors such as ease of placement, osseointegration, esthetics, peri-implant mucositis, marginal bone loss, mechanical flaws in design of implant/abutment connections, and mechanical failure of the loaded implant. The authors concluded that there was insufficient evidence to prefer one kind of surface modification over another and that the surface modifications performed comparably.

Furthermore, Xuereb *et al.* reviewed the current coatings investigated for dental implants, which include "carbon, bisphosphonates, bone stimulating factors, bioactive glass and ceramics, fluoride, [hydroxyapatite], calcium phosphate, and titanium nitride."[29] The

coatings improved the chemical and mechanical properties for dental implants. The most common coating techniques were plasma spraying and hydrocoating. Carbon coating promoted osteoblast adhesion on nickel-titanium alloys. Bisphosphonates could inhibit osteoclasts and preserve bone quantity. Fluoride was identified for selective osteoblast differentiation. HA was the most commonly used coating for dental implant surfaces. The only modifications reviewed that were on the market were fluoride coatings (Osseospeed), HA coating (Restore), and titanium nitride (IonFusion).

Liu *et al.* evaluated four different commercial dental implant surfaces (3i Nanotite®, Astra Osseospeed®, Nobel Biocare TiUnite®, and Straumann SLActive®) that reportedly made up 85% of the dental implant market.[30] The cell adhesion of primary mouse alveolar bone cells on these surfaces was also investigated. The group examined specifically the thread's valley, flank, and top, which was from the medial most to lateral most sections of the implant. For Astra and 3i systems, all three parts had equal roughness respectively. For Nobel implants, the roughness was flank>valley>top, and for Straumann implants, the roughness was flank > top > valley. The overall implant surface roughness ranking from highest to lowest was Astra > Straumann > Nobel Biocare > 3i. After 48 hours of culturing, primary cell adhesion was highest for Astra and Straumann. 3i had significantly less cellular confluences, and Nobel Biocare had the least cell adhesion overall. Implants manufactured by Nobel Biocare had the least amount of titanium based on EDX spectra as well. This may show that overall surface roughness on all portions of the dental implant and titanium was needed for improved cell adhesion.

2.3 Nanotechnology, Nanomedicine, and Nanotubes

Nanotubes have been used for many purposes: gene therapy, antibiotic delivery, vaccine development, siRNA delivery, gene silencing, etc.[31, 32] Nanomedicine has concentrated around the use of carbon nanotubes (CNT) for drug delivery.[31] Changing the diameter of the carbon nanotubes has been shown to be directly related to the strength of stacking of conjugated molecules and allows an operator to control the release rate of a drug or molecule of choice.[33] As with tubular objects, when the apex or tip of the tube was cut off, the nanotube could serve as a reservoir of any matter for potential drug delivery.[31]

Carbon nanotubes have also been studied as a drug carrier, with platinum compounds as prodrugs that resist substitution. Studies show functionalized single-walled carbon nanotubes could enter a cell through clathrin-dependent endocytosis.[33] The drug was only released after cellular internalization.[33] The high surface area of the nanotubes was key to heavy packing of drugs.[34] This in turn lent to a relatively small amount of drugs needed for the desired effect, as a greater percentage of drug was delivered with nanotubes than the drug alone.[35] The drug then had prolonged blood circulation, increased cellular permeability, and rapid clearance from the reticuloendothelial system.[34] Drugs became more hydrophilic after linkage to nanotubes, while maintaining its desired effects on targets.[34] The amount of linking of a molecule of interest to nanotubes and the diameter of nanotubes could be controlled and altered in multiple ways, such as altering pH and anodization time.[34, 36] Release of the molecule of interest could also be controlled by altering the pH.[37] In cancer cell therapy studies with doxorubicin, release went from 15% to 40% when pH decreased from 7.4 to 5.5, and was more stable in delivery.[37, 38]

Nanotubular treatment of implants has been studied extensively, as it has been shown to be economic, efficient, specific, and enduring.[33, 34] Previous studies have used gel layers to over coat an antibiotic or protein on titanium surfaces to create a better reservoir and barrier against degradation.[39] The disadvantage was that the multiple gel coatings must be degraded for the antimicrobial proteins to become available.[39] Moreover, long-term antibacterial effects of these coatings have been limited.[40] The emergence of antibiotic resistant microorganisms and the gradual degradation of the antibiotics also reduce the efficacies of the antibiotics.[10]

2.4 Titanium Nanotubes via Anodization

Nanotexturing of implant surfaces, particularly titanium oxide nanotubes (TiO_2-Nt), has attracted tremendous attention in the last decade. Nanostructured surface on dental implants have shown a positive correlation with improved osseointegration in as little as twelve weeks.[6]

Nanotube formation techniques may include chemical vapor deposition, template-assisted method, hydrothermal treatment, and electrochemical anodization.[41, 42] Anodization is a popular, economic, efficient, and convenient method of titanium oxide (TiO_2) nanotube formation on titanium plant surfaces.[36] The process uses a "conventional two-electrode cell" with titanium as the anode.[10] The nanotubes that are formed via anodization are also better organized compared to other methods. Titanium is treated for a set amount of time (about 1 hour) and may be etched and immersed in solutions with desired modification molecules or elements to bind onto or become incorporated into the titanium nanostructure.[10] Increasing the anodization time with the same acid concentration results in increased nanotube diameter.[36]

The methodology of the novel TiO_2-NT-Ag fabrication has been established in Dr. Shokuhfar's lab, and the test samples from their studies are depicted in Figure 1.[43, 53,104] She has published many articles related to this topic. In this method, Ag was embedded into the Nt resulting in more stable bonding between Ag and Nt. This novel Ag-Nt bonding may create a slow, constant and controlled release of Ag ions to achieve bactericidal activity. The TEM photo confirms the presence of silver within the nanotubular structure. At

present, limited information is available regarding the optimum Ag concentration used to prepare TiO_2-Nt-Ag surfaces to achieve the bactericidal effects.[21] Studies have shown that silver release from nanotubular titanium is logarithmic per 0.5M increase of silver solution used during preparation of TiO_2-Nt-Ag surfaces.[21]

Figure 1. FESEM and EDX from previous anodization protocol. (A. TEM picture depicting the presence of Ag inside (black arrow) and outside (white arrow) nanotubes, B. EDS analysis depicting the presence of Ag element (black arrow) on the nanotubes)[104]

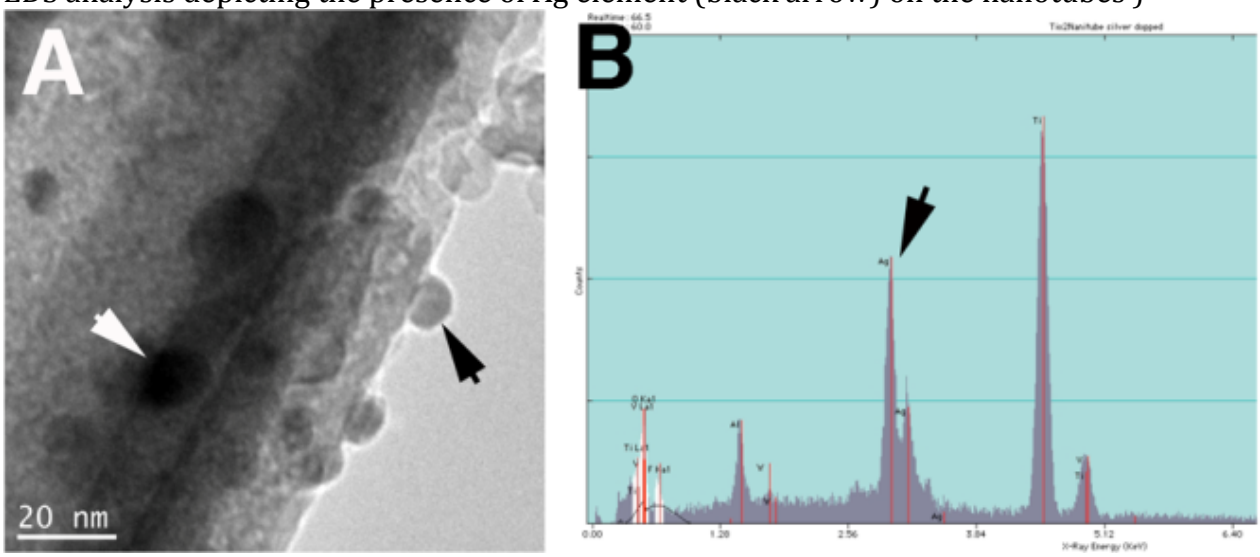

2.4.1 Antimicrobial Potential of Nanotubes

Nanotubular surfaces are valuable for various reasons. Singh *et al.* examined the influence of nanoscale morphology of titanium thin films on the attachment of *Escherichia coli* and *Staphylococcus aureus.* For the surface characterizations, the increase of surface roughness decreased the water contact angle and increased the surface energy.[44] Following Wenzel's law, the roughness contributed to increased hydrophilicity to the surface.[45] For the bacterial attachment studies, as the surface roughness increased, there was a reduction of bacterial biofilm colonization. Therefore, it was suggested that that surface roughness

treatment was inhibitory to bacterial growth.[44] Proteins accumulated more around the roughened surface and may have become a barrier, inhibiting bacterial adhesion.[45] In a study by Frodj *et al.*, saliva increased the biovolume of biofilm and promoted the adhesion of bacteria to nanoporous TiO_2 coatings.[46] Intraoral conditions may also affect the behavior of surfaces and bacterial adhesion.

In another study, macrophages cultured on nanotextured titanium had rounder morphologies and less colony spreading than on smooth titanium surface.[36] This may indicate a decreased inflammatory response for the nanotextures surface. In addition, heat treatment of titanium significantly reduced bacterial adherence to the same nanotextured surface, and titanium surfaces with larger diameter nanotubes promoted less adhesion by live bacteria.[47] Treating titanium to both conditions resulted in a reduction in bacterial adherence, especially with 80 nanometer diameter nanotubes in *in vitro* studies.[46] Nanotubular surface treatment of titanium had no obvious cytotoxicity when compared to smooth titanium in *in vitro* studies on rat osteoblasts.[48] The mechanical interlocking associated with nanostructure may have enhanced osseointegration *in vivo*.[48] In some animal studies, nanotubes generated from anodization were shown to accelerate osseointegration.[49] The structure of the nanotubes was observed to be biomimetic of the "nanoscale features of bone."[36, 50] Titanium nanotubes were also found to be conducive to nanostructured hydroxyapatite growth *in vivo* and allowed many functions of osteoblasts such as mineralization and extracellular matrix secretion.[40]

2.4.2 Biocompatibility of Nanotubes

Increasing the diameter of the titania nanotubes could also induce stem cell elongation and ensuring differentiation.[25] In a study by Oh *et al.* 2008, anodization was used to create nanotubes of various diameters (30, 50, 70, 100 – nm). These nanotubular surfaces were then coated with equal amounts of proteins. Human mesenchymal stem cells were then plated on these surfaces and observed intermittently for 3 weeks. Under the FESEM, it was shown that initially, the stem cells were much more densely packed on the 30nm compared to the 100nm, and as the nanotube diameters increased, the stem cell elongated 10x more than the 30nm groups in order to reach more proteins. Over time, the stem cells caught up in cell density among all groups. The physical stress of elongation may have induced the early differentiation of the stem cells into osteoblastic-like lineage that was observed. This was encouraging as a way to control cellular growth and differentiation based on titanium morphology alone, which is more predictable.[51] However, Park *et al.* found that a smaller nanotube diameter (15nm) promoted stem cell adhesion and attachment.[52]

Titanium nanotubes could also affect the behavior of osteoblasts.[53] In a study by Shokuhfar *et al.*, commercially pure titanium was used to create both amorphous and crystalline titanium nanotubular surface. Cell density was measured to be greater on the nanotubular surface compared to the smooth commercially pure titanium. The crystalline nanotubules also enhanced cell growth better than the amorphous nanotubes. The smaller diameter nanotubes also had greater cell density. In addition, the focused ion beam analysis showed that the cells extended and not only used the nanotubes as physical

anchors for migration, but also migrated into the crystalline nanotubes. This intimate contact between cells and nanotubular surface may be promising as an improved stronger bone-to-implant contact surface and osseointegration.

2.5 Peri-implantitis and Peri-mucositis

Biologic implant associated complications include peri-implantitis and mucositis.[54] Mucositis occurs when the peri-implant mucosa exhibits inflammation, and could be reversed with proper treatment.[54] Peri-implantitis, on the other hand, is defined as "an implant disturbance due to inflammation, with end result of irreversible bone resorption and inflammation." It can be triggered by peri-implant lesions, aggressive bacteria, excessive mechanical stress, and corrosion.[54]

2.5.1 Diagnosis of Peri-implantitis

According to Lindhe *et al.*, peri-mucositis is diagnosed as the erythema and swelling of soft tissue and bleeding upon probing.[55] Peri-implantitis has the same clinical manifestations as peri-mucositis, in addition to surrounding bone loss.[55] Peri-implantitis was observed in a study with a follow-up of 1 year in 28-56% of the subjects, and in 12-43% of implant sites. The risk factors for this disease included poor oral hygiene, smoking, and history of periodontitis. The treatment of peri-mucositis could potentially be resolved by using non-surgical methods such as improved oral hygiene, mechanical removal, and oral rinses. Peri-implantitis was shown to have unpredictable results by nonsurgical treatment alone, and surgical treatments focused on debridement and decontamination of surfaces.[55] Due to the lack of evidence, regenerative procedures for these sites was neither supported nor refuted as well. Heitz-Mayfield also suggested to regularly probe (0.25N) around implants to have baseline values and monitor bone levels over time, which contrary to popular opinion, "would not damage" the peri-implant tissues.[56]

Derks and Tomasi conducted a systematic review to look at the epidemiology of peri-implantitis.[57] Fifteen articles describing 11 studies were used, although they had slight variations in definitions of peri-implant conditions, had different baseline time points, and had various function times of between 3.4-11.0 years. For peri-mucositis and peri-implantitis, the prevalence was 19-65% and 1-47%, respectively. The weighted mean value were 42.9% (95% CI 32-54%) and 21.7% (95% CI 14-30%), respectively. The reviewers noted that the various studies used had different assessments for the peri-implant conditions and lacked qualitative descriptions of severity of disease. There was lack of consensus in the evidence. Jung *et al.* also noted that peri-implantitis and soft tissue complications occurred in 9.7% of the single crowns over a 5 year observation period.[2]

Radiographically, peri-implantitis presents like a well-demarcated "saucer" around the implant and can be confirmed by bleeding upon gentle probing, suppuration, radiographs, and biochemical and bacteriological markers.[54] The condition was more likely to develop when there was poor bone quality or poor surgical technique that results in overheated bone.[54] Current treatment modalities include guided bone regeneration for walled lesions as well as citric acid and CO_2 laser treatment. The goal is to decontaminate the area and reestablish the osseointegratable properties of the implant surface.[54] When an implant is initially placed, the body reacts as if the implants is a foreign body.[36] Macrophages and fibroblasts are recruited to cover the implant with soft fibrous tissue.[36] Microorganisms also compete for the new implant surface and thus cause a "race for the surface."[58] Peri-implantitis is hard to control as the biofilm that adheres is hard to remove,

and an effective treatment recommended by studies is the prevention of initial bacterial biofilm formation.[40, 59]

2.5.2 Treatment of Peri-implantitis

Esposito *et al.* conducted a Cochrane systematic review of the treatments for peri-implantitis.[8] Only 9 studies were selected, and all studies had various bias risks and follow-up between 3 months to 4 years of adult patients. Nonsurgical adjunctive therapy included local antibiotics, air abrasive devices, and lasers, in addition to manual debridement, and they all showed various degrees of improvement. Follow-ups of more than 1 year reported peri-implantitis recurred in 100% of the cases. Surgical intervention included flap surgery and plastic curettage with either ridge augmentation - to fill the defect, not to treat the infection- or laser debridement, and both techniques were equally effective as each other. Xenografts performed better than allografts, although the studies were judged to have high risks of bias. None of the studies compared surgical versus nonsurgical techniques. Due to the lack of evidence, the authors could not conclude which technique was most effective, but suggested that the treatment modalities reviewed could be effective. Larger more controlled studies were needed to provide a consistent, effective treatment results.

Most contemporary implants have platform switching to elongate the distance between the bone and the oral seal, thus decreasing the chances for peri-implant lesions.[54] The bacteria that are involved in peri-implantitis are mostly rods and Gram-negative anaerobes commonly associated with periodontitis. The species include *Prevotella intermedia, P. gingivalis, Aggregatibacter actinomycetemcomitans, Bacteria forsythus,*

Treponema denticola, Prevotella nigresens, Peptostreptococcus micros, and *Fusobacter nucleatum*.[54] Lipopolysaccharide, a component of the Gram-negative bacteria, bound well to many biomaterials and "[may stimulate] macrophages to secrete osteoclast-activating cytokines.[60] Rough surfaces may also enhance bacterial attachment and colonization.[54] Multiple contributing factors are theorized to be involved with bacterial attachment on peri-implant areas.

As previously mentioned, the transgingival section of an implant is most vulnerable to bacteria.[61-63] Bacterial attachment to an intraoral surface has been theorized to occur in a distinct order of events. Bacteria are transported to a surface by Brownian movement; initial, weak, reversible adhesion occurs; bacterial attachment become definitive (though it can be still removed with shear forces); and mature bacterial colonization ensues with permanent bonds.[61] Methods to create and enhance the antimicrobial capacity of titanium have been explored, such as UV illumination, dry ion implantation on titanium surface, incorporation of antibiotics on the surface, and salt anodization.[61] Bacteria may invade from adjacent skin and mucosa through external fixture pins as well, and implants are susceptible to bacterial invasion throughout their life time of use.[64] Besides preventing initial seepage of bacteria, prevention of primary attachment of bacteria is key to preventing biofilm formation.[10] *In vitro* studies have shown that bacteria were able to create pitting corrosion on titanium surfaces, which reduced the mechanical properties of implants.[65] The corrosion resulted from passage of electron from titanium to bacteria, especially when sulfur is involved.[65] It had been suggested that it was difficult and maybe

ineffective to treat bacterial invasion around implants and much easier to prevent biofilm formation.

2.6 *Porphyromonas gingivalis*

P. gingivalis is a prominent periodontal pathogen that is also associated with periimplantitis.[54] It is also a late colonizer of intraoral dental plaque.[66] Dental plaque is composed mainly of bacteria in an extracellular matrix of salivary glycoproteins and polysaccharides. The plaque develops into a biofilm in recognizable sequence. The proteins and polysaccharides in the initial pellicle on the tooth provide receptors for initial bacterial colonizers such as *Streptococcus sanguis* and *Actinomyces* species. Once the bacterial attachment matures, bacteria starts forming microcolonies and coaggregates with other bacteria. This enables the binding of the late colonizers, including *P. gingivalis,* an asaccharolytic and proteolytic species.[66, 67]

The pathogen, *P. gingivalis,* produces virulent factors, such as adhesins (fimbriae), capsule, lipopolysaccharide, and extracellular proteases, that can modulate "host immune response, attachment, and degradation or cleavage of host cell proteins and surface receptors."[68, 69] Recent studies have shown that *P. gingivalis* can colonize the subgingival epithelium without overt disease.[68] However, once the body's inflammatory response is initiated, *P. gingivalis* is able to damage the host cells such as macrophages, neutrophils, fibroblasts, and endothelial cells.[68]

2.6.1 *P. gingivalis* vs. Titanium

In a study by Takanashi *et al.*, the authors concluded that the colonization of *P. gingivalis* and *P. intermedia* around dental implants in treated patients came from the patients' own natural teeth plaque.[70] The study had 12 patients that needed dental implant

treatment. Prior to implant placement, they underwent oral hygiene instruction to encourage good home care. The plaque samples around the patient's natural teeth and respective dental implant sites were taken 1 month prior to fixture installation (not for dental implant site), one month prior to abutment connection, 1 month after abutment connection, and 6 months after restoration use. The plaque was analyzed with polymerase chain reaction (PCR) to isolate strains and confirm presence of *P. gingivalis* and *P. intermedia.* Prior to treatment, the presence of *P. gingivalis* and *P. intermedia* was 85.4% and 60.0%. For the subsequent 3 time intervals, the presence of *P. gingivalis* was 63.7%, 58.5%, and 56.8%. PCR confirmed they were the same strains of *P. gingivalis* from the natural teeth plaque taken at baseline. The authors concluded that *P. gingivalis* around osseointegrated healthy dental implants must come from the patient's own oral flora. The authors did not report any pathology nor implant failures, and assuming this was true, another conclusion that could be drawn was that pathologic bacteria such as *P. gingivalis* and *P. intermedia* were naturally present around > 58% and >41%, respectively, of implant sites and did not necessarily cause harm from their presence alone.

Other studies have been completed to observe the attachment of *P. gingivalis* on titanium surface.[71-73] Kim *et al.* looked at the attachment of the pathogen on various sandblasted titanium surfaces to see how surface roughness affects bacterial attachment.[71] The authors of the study noted that from previously published literature, Mg-ions incorporated in titanium surfaces promoted a stronger initial cellular response and bone response, thus, the investigators incorporated Mg-ions onto half of the titanium samples via plasma source ion implantation. The XPS characterization of the surfaces showed the

Mg-ions formed oxides on the surface. The results showed that the sandblasted surfaces had significantly higher *P. gingivalis* attachment compared to the ground surfaces, and the Mg-ion surfaces had 2x and 1.5x more bacterial attachment on rough and ground surfaces, respectively, compared to non-Mg-ion surfaces. Prior to bacterial inoculation, half of the samples were also immersed in artificial saliva (filtered lemon juice) to simulate intraoral conditions, and all 4 kinds of surfaces had significantly increased bacterial attachment. The surface topography, surface chemistry, and surrounding environment were shown to work synergistically in promoting *P. gingivalis* attachment. Similarly, Wu-Yuan *et al.* examined *Streptococcus sanguis, Actinomyces viscosus,* and *P. gingivalis* attachment on titanium surfaces with different surface topography (smooth, grooved, and rough), and *P. gingivalis* was found to attach most to rough surfaces and equally well to both smooth and grooved surface. The authors observed under SEM that perhaps *P. gingivalis* attachment was strongly related its characteristic fimbriae, which was considered one of its virulent factors.[68, 72]

2.7 Silver & Implant Dentistry

Current uses of silver in dentistry are mainly for dental restorations as part of an alloy.[74] Its physical properties, especially its mechanical strengths, make it desirable as an alloy constituent. However, silver reacts with sulfur, chlorine, phosphorus, and their various compounds and forms tarnish and corrosion products.[75] Foods containing these compounds can also increase the corrosion of silver. Addition of palladium has helped prevent the rapid corrosion behavior of silver products in dental alloys.[74]

The antimicrobial properties of silver has been extensively investigated and published. Silver (Ag) has been used as an antibacterial agent that is incorporated in many dental and medical biomaterials.[10, 63, 76, 77] Ag has a broad antibacterial spectrum, good inorganic-derived stability, lower toxicity, high surface-area-to-volume ratio, and lesser possibility to develop bacterial resistance.[12, 63] It has a high efficacy at low concentrations and condenses well into the nanotube reservoirs.[10] Some experimental evidence suggests that silver coatings may even "enhance osteoblast proliferation, fibroblast attachment, and endothelial cell response."[10]

Ag nanoparticles can be incorporated into the walls of TiO2-NTs (nanotubes) by immersion in silver nitrate solutions and UV radiation.[10] The concentration of Ag incorporated could be controlled by altering the concentration of the $AgNO_3$ solutions and immersion time. The goal of most silver nanotube studies is to observe a lasting antibacterial effect of nanotubes (>30 days, past the initial healing phase) while having minimal cytotoxicity of host cells. Existing research suggest that much less bacteria

adhered to silver-treated titanium than to smooth titanium surfaces.[10] Silanization is another way to produce titanium nanotubes but does not deposit silver well.[77] Anodization is also used to create silver titanium nanotubes.[36]

2.7.1 *In vitro* studies on Nanotubular Titanium

In a recent article, Zhao *et al.* introduced a new technique to fabricate TiO_2-Nt loaded with Ag nano particles. In their study, annealed Nt was soaked in $AgNO_3$ solution and results showed that the modified Nt-Ag surface was bactericidal during the first several days.[10] They also suggested that Nt-Ag maintained their antibacterial properties for 30 days. This study showed the antimicrobial potential of silver topically incorporated into titanium nanotubes. However, some cytotoxicity to osteoblast cells was observed. It was proposed that this hazardous cytological phenomenon was due to rapid leaching of Ag to the cells culture medium. If the silver were incorporated as part of the entire titanium nanotubular structure, then the silver may have decreased leaching and increased biocompatibility.

In another study by Zheng *et al.*, silver nanoparticles of 10nm in size were incorporated into a titanium nanostructured surface via plasma immersion ion implantation. The surfaces were then treated separately with *Streptococcous mutans, P. gingivalis, and Candida albicans*.[63] The study showed 93.99% of *S. mutans,* 93.5% of *P. gingivalis*, and 89.78% of *C. albicans* were killed on the surface. Furthermore, the study plated mouse calvaria-derived osteoblast cells on the surfaces. The number of osteoblasts grown on the silver treated surface was comparable to the number on the non-silver

treated surface. The cells also had more pseudopodia extensions across the nanostructured surfaces, which the authors attributed to the physical properties of nanostructured surfaces. The study showed promise for silver induced microbial inhibition on titanium surfaces that were treated with thermal oxidation for a nanostructured surface.[18]

Another study by Vargas-Reus *et al.* evaluated the antimicrobial activity of various nanoparticulate metal oxides against the peri-implantitis pathogens, *Prevotella intermedia, P. gingivalis, Fusobacterium nucleatum, and Aggregatibacter actinomycetemcomitans.*[78] Although the study focused mainly on ZnO, the authors also tested various other nanoparticles (50-100nm in size) for potential minimum inhibitory concentration and minimum bactericidal concentration. The various bacteria were grown in medium with the each kind of nanoparticle at various concentrations (100, 250, 500, 1000 and 2500 **μ**g/mL), and optical density of the bacterial suspension was assessed after 48 hours of incubation. The results of studies showed that the antimicrobial activity of the nanoparticles in descending order were as follows Ag >Ag + CuO composite > Cu_2O > CuO > Ag + ZnO composite > ZnO > TiO_2 > WO_3. In some instances, the nanoparticles were bactericidal, and even with reduced initial concentration of the nanoparticles, over time the medium became bactericidal. When inoculated with *P. gingivalis* culture, Ag alone had MIC and MIB of both 250 **μ**g/mL, and when combined with other particles (Ag + CuO and Ag + ZnO), the MIC and MIB were <100 **μ**g/mL and <100 **μ**g/mL, and <100 **μ**g/mL and 250 **μ**g/mL, respectively. This showed the high antimicrobial potential of silver in small amounts against *P. gingivalis.*

2.7.2 Silver's Mechanism of Action

Multiple mechanisms of action have been proposed to explain the intracellular behavior of silver. *In vitro*, silver has been shown to bind to microbial DNA and halt metabolic enzymes of cellular respiration, namely sulfur, oxygen, and nitrogen electron donor groups of the electron transport chain.[79, 80] When incorporated into nanotubes, silver could also be released into the surrounding environment. [81] In a study by Matteis *et al.*, silver nanoparticles were purposefully internalized in HeLa and A549 cancer cell lines, and a fluorescent probe was used to observe silver's mechanism of action.[82] After the silver nanoparticle entered the eukaryotic cell, the lysosomes phagocytized the particles and released Ag^+ ions into the cytosol. The elevated concentrations of Ag^+ ions in the cytosol altered the mitochondrial membrane potential, which impaired normal cell metabolism, and induced apoptosis via oxidative stress. The authors postulated that this could be prevented with addition of metal chelating agents to bind to the silver ions. The cytotoxicity of silver was also observed to be dose dependent and dependent on the release of silver ions into the cytosol. Conversely, the authors observed that Ag^+ ions in the extracellular matrix had negligible cytotoxicity effects.

Atl *et al.* hypothesized that the cytotoxicity management of silver could be accounted for by the natural structure of host cells.[76] Eukaryotic cells were larger targets, with more structure and genetic redundancy that lent it stronger against the silver mechanisms of actions. A greater concentration of silver would be needed for significant cytotoxic effect, thus silver may have a relatively high therapeutic index.[76] Silver ion also did not seem to linger around tissue, which stopped the opportunity for cytotoxicty and

potential side effects.[63] Osteoblast gene expression and colony formation have also shown to be more extensive on silver-titanium surfaces than smooth titanium surfaces. [63]

Few studies exist to find an optimum silver coating concentration that both resists biofilm formation while exhibiting low to no cytotoxicity.[10] Zhao *et al.* found that silver released from nanotubular titanium has been shown to be logarithmic per 0.5M increase of silver.[10] The minimum inhibitory concentration may be between 0.5M-1.0M. Their study had topical application of silver particles onto titanium nanotubes and used *Staphylococcus aureus* as their system, which is a Gram-positive bacteria often associated with skin infections and respiratory disease. This study sought to find an optimum effective inhibitory concentration of silver incorporated in titanium nanotubes, via anodization.

3 METHODS

3.1 Preparation of Samples

Commercially Pure Ti (CP-Ti) foil with 0.25 mm thickness, 25 X 25 cm dimensions and 99.7% purity (Sigma Aldrich, St. Louis, MO, USA) was used in this experiment. The schematic of the protocol is depicted in Figure 2. Before electrochemical anodization to form silver deposited nanotubes, CP-Ti foil was cleaned by sequential sonication in ethanol for 15 minutes and deionized-water (DI-water) for 15 minutes followed by air drying. After anodization, the surfaces were cut into 5mm by 5mm for the bacterial attachment assay. There were 6 different kinds of surface groups fabricated in this study: commercially pure titanium surface (CP-Ti), titania nanotubular surface with no silver (TiNT), and 4 kinds of silver-embedded titania nanotubular surfaces (TiNT-Ag-0, TiNT-Ag-5, TiNT-Ag-10, and TiNT-Ag-30). The number behind the Ag denotes the number of seconds involved in the reverse polarization process of intentional silver deposition in the fabrication of the silver-embedded titania nanotubular surfaces. For every assessment, the CP-Ti served as a positive control, and the TiNT surface served as a negative control. The bacterial portion of this study was presented at the 2015 IADR Annual Session.[83]

Figure 2. Diagram of the Workflow of the Project

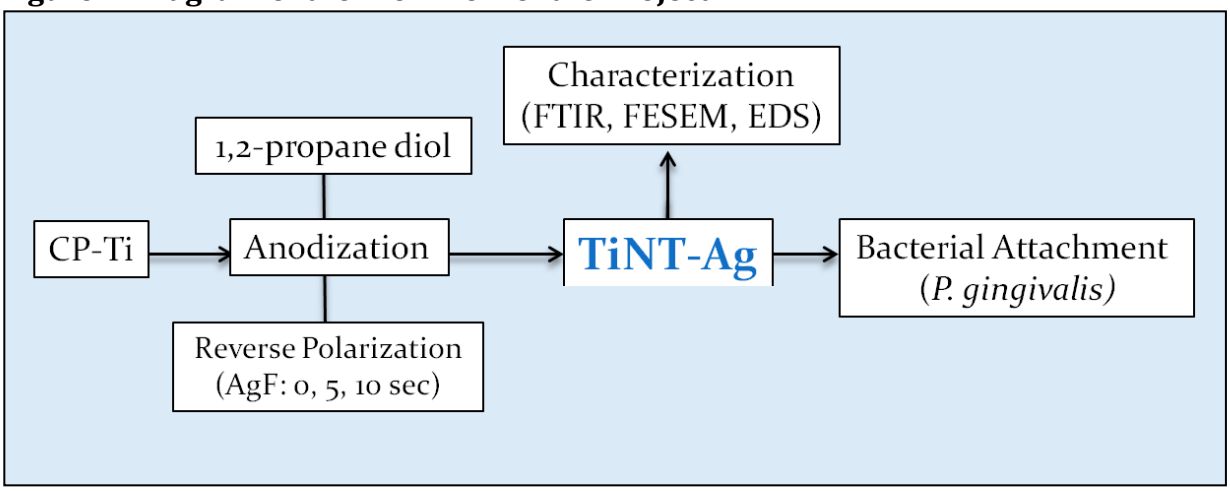

3.1.1 Anodization

For this experiment, the titanium surfaces were the anode as depicted in Figure 3. Graphite served as the cathode. The methodology of TiNT formation via anodization has been established in the Dr. Shokuhfar's lab.

Figure 3. Diagram of the Anodization Technique

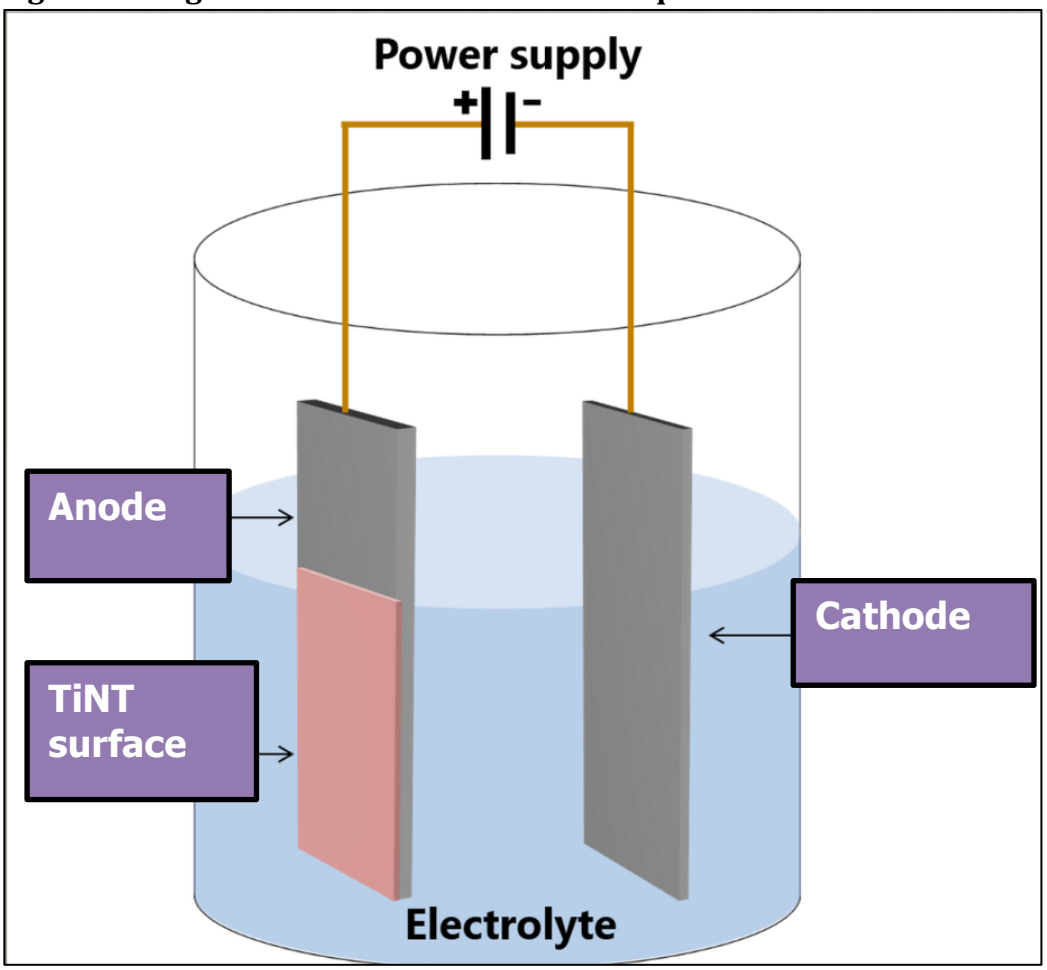

Electrochemical anodization for fabrication of silver nanoparticle-embedded TiO_2-nanotubes (TiNT–Ag) was carried out at room temperature with a variable reverse polarity duration including 0, 5, 10 and 30 seconds reverse polarity to incorporate different amounts of silver. The anodization process consisted of the following steps:

(1) Preparing the electrolyte composed of 20 vol% H_2O, 80 vol% 1,2-propane diol, and 0.66wt% AgF. ;

(2) Ti samples are used as the working electrode (positive terminal) and the graphite rods are used as the counter electrode (negative terminal). Both electrodes are submerged in the electrolyte.

(3) Energizing the circuit at 20V for a period of 4 hours for step one

(4) De-energizing the circuit and switch the polarity of the apparatus so that the titanium is now connected to the negative terminal and the graphite is connected to the positive terminal;

(5) Re-energizing the circuit at 20V for 5, 10 and 30 seconds to dope desired level of silver into/on the nanotubes; and

(6) After anodization, the samples were sonicated in ethanol for 2 minutes, then washed with deionized water followed by air drying.

For fabrication of non-silver embedded nanotubes, anodization was performed at room temperature in an electrolyte composed of 0.3 wt% NH_4F, 3 vol% H_2O in ethylene glycol. During the first step, anodization was performed at 90V for 1 hour. After anodization, the nanotubes were delaminated from the surface by first sonicating in 2-propanol for 15 minutes, then in DI-water for 15 minutes followed by washing with DI-water and then air drying. Then the delaminated sample was again processed through anodization at 90V for 30 minutes. After anodization, the treated samples with electrolyte were left in air for 2 hours. Then the samples were washed in ethanol first for 5 minutes,

then with DI-water followed by air-drying. For 0 seconds reverse polarity, samples were not subjected to the second step.

After anodization, samples were washed with DI-water, air dried, and put in new disinfected petri dishes. The samples for bacterial attachment were put in sterilization bags and underwent ethylene dioxide gas sterilization.

3.2 Surface Characterizations

3.2.1 Fourier Transform Infrared Spectroscopy (FTIRS)

Surface composition of all surface types was observed using diffuse reflectance FTIR spectroscopy (FTIR, Nicolet, Madison, WI, USA) and an EDX attachment to the JEOL JSM-6320F FESEM. FTIR spectra were performed with non-anodized CP-Ti as a background sample using the previously established protocol.[47] Prior to conducting FTIR analyses, each sample was kept inside the FTIR chamber for 1 hour in order to stabilize the internal conditions and optimize signal to noise ratio. H_20 and CO_2 were purging gases of the system. The scanning resolution used was 2 cm^{-1} with 512 scans over the range of 400-4000 cm^{-1}. FTIR spectra were analyzed with linear background and deconvoluted using Gaussian-Lorentian peak shape function with spectral peak-fitting software.

3.2.2 Field Emission Scanning Electron Microscopy (FESEM) & Energy Dispersive X-ray Spectroscopy (EDS)

Surface external morphology was investigated using field emission scanning electron microscopy (FESEM, JSM-6320F, JEOL, Musashino 3-chome Akishima Tokyo, Japan).[50] After preparing the samples, they were mounted on an aluminum stub with the help of double sided conductive copper tape for imaging. FESEM images were obtained with acceleration voltages of 10 KV, and working distance 15. Noran Voyager Energy dispersive X-ray system with a light element X-ray detector (15mm WD) and an Autrata Back Scatter Detector was used to investigate the presence of elemental composition on the samples. The protocol by previous nanotubular scientists was used.[42] For EDX, random locations from the sample surface were analyzed. For the suspected elements, two times

the emission energy of the element with the highest emission energy was recommended. Emission energies of titanium (Ti) was 4.508 keV.

3.2.3 Water Contact Angle (WCA)

Water contact angles were recorded for wettability analysis of each sample. The protocol was adopted by Butt *et al.*'s group.[42] Goniometer was used to measure the WCA of all the samples for days 0, 1, 4, 6, 11, 18 with 26. 5 µl of DI-water placed on the each sample, which was then analyzed using Image-J software. Prior to each WCA measurement, samples were blow dried with N_2 gas.

3.2.4 White Light Interferometry (WLI)

WLI (NewView 6300, Zygo Corporation) was used to carry out surface roughness measurements of each surface group for average roughness values (RA) per protocol by Butt *et al.*'s group.[42] Due to the morphology of titanium nanotubes, light did not propagate to the bottom of the TNT structure, therefore accurate roughness measurements could not be taken.

3.3 *Porphyromonas gingivalis* Biofilm Attachment

3.3.1 *In Vitro* Attachment Assay

The protocol used was adopted and modified from previous studies by Valentim *et al.* 2014 and Roberts *et al.* 2002. [44, 46] *P. gingivalis* was grown at 37°C in Todd-Hewitt broth (THB) with 0.001% Hemin & 0.0001% Vitamin K1 in an anaerobic chamber filled with mixed gases (Praxiar, 5% CO_2, 10% H_2, 85% N_2). Subsequently, 1% of 2-3 days old culture was inoculated into fresh growth medium (THB with 0.1% Hemin & 0.01% Vitamin K1) at 37°C for 48hr in the chamber. The cells were then harvested by centrifugation at 10,000 rpm for 3min, washed, resuspended in PBS (pH=7.4, pre-treated in anaerobic chamber to reduce O_2), and adjusted to OD_{550} =0.2 (~$7x10^7$ CFU/ml) by adding PBS. A drop of suspension was examined under a light microscope to ensure bacteria purity. The cell suspension was then mixed at a 1:6 ratio with fresh growth medium to desired CFU based on OD_{550}. Each titanium sample was placed into a single well of the 24-well culture plate, with 2ml of the bacteria culture mix added into each well. The plates were then incubated in the anaerobic chamber at 37°C for 12 hours. Afterwards, the titanium samples were washed gently with 1ml PBS and transferred into wells of new plates. The plates were allowed to dry at 37°C dry for 20 minutes. For quantitation of biofilm, 0.5ml of Crystal violet (0.05% solution) was added to each titanium surface and left standing for 15 minutes. The titanium samples in the wells were then washed four times with 1ml PBS per wash and the dried at 37°C dry for 15 minutes. The crystal violet stain retained on titanium surfaces was extracted with 300µl of EtOH (90%). 200µl of the content was placed into a new 96-well plate to measure OD_{550} with a spectrophotometer.

3.3.2 Live/Dead Stain

The proportion of live or metabolically active *P. gingivalis* cells (fluorescent green) and dead or inactive cells (fluorescent red) was performed using the Live/Dead BacLight bacterial viability kit (Molecular Probes – L7012, Invitrogen, USA).[73, 84] The live/dead stain was prepared following the protocol from the manufacturer. For Live/Dead stain analysis, 6 types of surfaces were tested: CP-Ti, TiNT, TiNT-Ag-0, TiNT-Ag-5, TiNT-Ag-10, and TiNT-Ag-30. After the surfaces had 12 hours incubation with *P. gingivalis*, the surfaces were sequentially treated with staining reagents and examined under the microscope, one sample at a time. Briefly, 1.5 μL of staining component A (SYTO 9) and 1.5 μL of staining component B (propidium iodide) was mixed in 1 mL of sterile 1% PBS – pH 7.4 (Invitrogen, USA). One hundred microliters of each reagent mixture was used to cover each sample and then incubated for 15 minutes at room temperature in darkness. The fluorescence emission was examined under a fluorescent microscope (Leica DMRE microscope, Wetzlar, Germany) in combination with the image processing software (Image J, http://rsbweb.nih.gov/ij/). In each specimen, three fluorescent microscopic images of randomly selected sites of the disc were captured with a digital camera (Nikon, Japan) that was connected to the microscope. Live and dead cells in the same microscopic field were viewed separately with different fluorescence filters (cyan and green excitation) at 10X, 20X, and 40X. The areas covered by dead cells (fluorescent red), viable cells (fluorescent green) and total cells were evaluated with the image analysis software.

3.3.3 Field emission scanning electron microscopy

After the plates were rinsed following P. gingivalis incubation, they were treated with glutaraldehyde solution to fix for FESEM. Like the protocol for FESEM prior to bacterial attachment, FESEM images were obtained with acceleration voltages of 10 KV, and working distance 15. Prior to imaging the bacterial attachment samples, all samples were coated with about 5 nm of Au/Pd coating. No Au/Pd coating was done on non-bacterial attached samples. Presence or absence of bacteria on the surfaces was determined.

3.4 Statistical Analysis

The cells viability and live/dead counts data from all control and experimental TiNT–Ag groups were statistically analyzed using one-way ANOVA. Tukey's HSD test was used for subsequent pairwise comparisons within groups. Two-sample independent t-test was performed for comparisons between time points. Statistical analysis was performed with the SPSS software (SPSS – Statistical Package for the Social Sciences, Inc., Chicago, IL, USA) with significance level of 5% (p-values<0.05).

4 RESULTS

4.1 Surface Characterizations of Titanium Samples

4.1.1 Fourier Transform Infrared Spectroscopy (FTIR) Analysis

Fourier Transform Infrared Spectroscopy of the six different sample surfaces (CP-Ti, TiNT, TiNT-Ag-0, TiNT-Ag-5, TiNT-Ag-10, and TiNT-Ag-20 are shown in Figure 4. Characteristic absorption peaks for H_2O were observed at 3600-3900 cm^{-1} and 1400-1900 cm,$^{-1}$ and for CO_2 at 2200 – 2400 cm^{-1}. Additionally, a broad peak was observed in all the samples in the range of 500 – 1100 cm^{-1} wavenumber. Similar FTIR spectra were observed for 5, 10, and 30 seconds reverse polarity samples. For 0 seconds reverse polarity, a broad absorption peak is observed between 2400-3400 cm^{-1}.

Figure 4. Fourier transform infrared spectroscopy analysis.

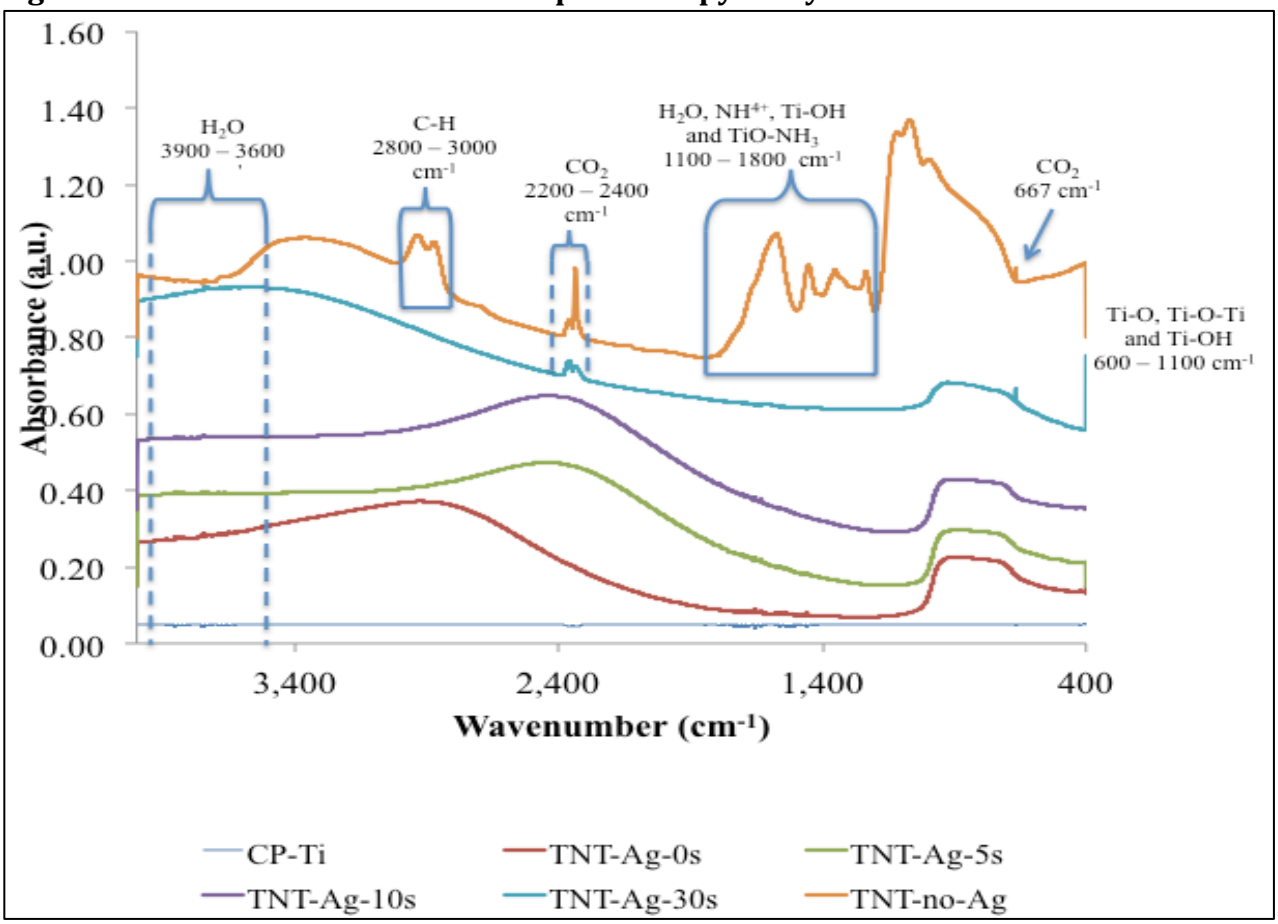

4.1.2 Field Emission Scanning Electron Microscopy (FESEM) & Energy-Dispersive X-ray Spectroscopy (EDX)

Field emission scanning electron microscopy and energy dispersive x-ray spectroscopy of the six different sample surfaces are shown in Figure 5. For each sample, the FESEM image was at 40,000x magnification and was superimposed on the blank portion of the sample's EDX reading, and each of the six samples was labeled accordingly in Figure 5. FESEM depicted a smooth surface for CP-Ti, and the EDX was suggestive of titanium and little to no contamination of the surfaces.

Figure 5. Field Emission Scanning Electron Microscopy & Energy-Dispersive X-ray Spectroscopy Results

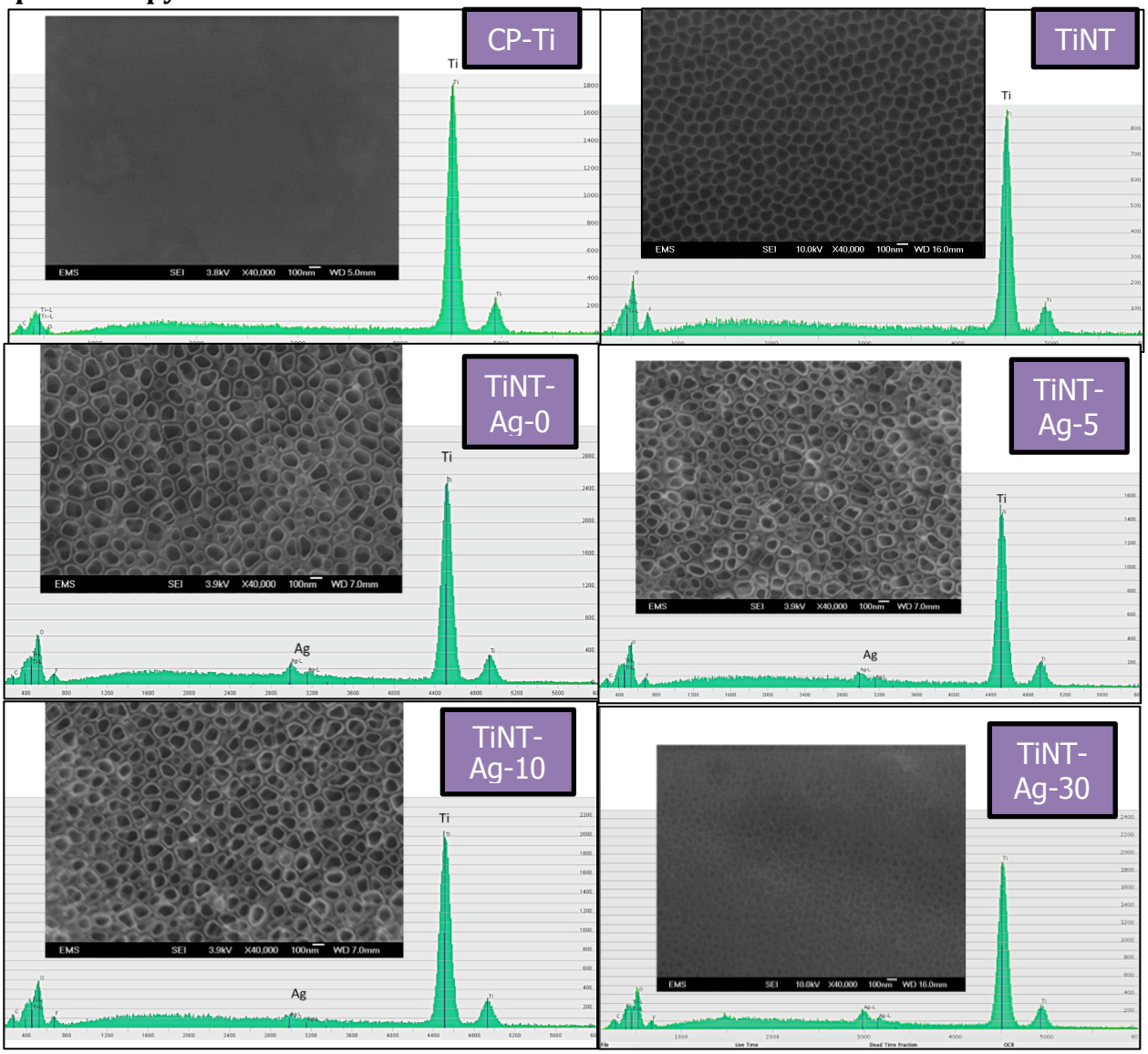

As seen in Figure 5, all nanotubes samples yielded the same diameter nanotubes of 80 – 100 nm from FESEM. Clear pore openings were observed for all nanotubular samples. EDX spectra proved the presence of silver along with other known elements including titanium, oxygen, carbon and fluoride for TiNT-Ag-0, TiNT-Ag-5, TiNT-Ag-10, and TiNT-Ag-30 seconds reverse polarity samples.

4.1.3 Water Contact Angles (WCA)

Goniometric readings of the WCA for all the 6 surface types (CP-Ti, TiNT, TiNT-Ag-0, TiNT-Ag-5, TiNT-Ag-10, and TiNT-Ag-30) were taken on days 0, 1, 4, 6, 11,18, and 26, and the WCA are recorded in Table 1.

Table 1. Water Contact Angle Readings for all Groups over 26 days

	CP-Ti	TiNT	TiNT-Ag-0	TiNT-Ag-5	TiNT-Ag-10	TiNT-Ag-30
Day 0	61°± 3	5°± 0	7°± 2	8°± 2	9°± 5	6°± 2
Day 1	69°± 0.9	5°± 0	17°± 3	30.°± 6	20.°± 5	12°± 4
Day 4	71°± 6	5°± 0	16°± 3	30.°± 4	22°± 3	21°± 3
Day 6	71°± 7	9°± 1	13°± 2	24°± 6	24°± 4	22°± 5
Day 11	77°± 4	7.°± 2	25°± 4	24°± 2	23°± 3	25°± 10.
Day 18	74°± 10	5°±0	20.°± 3	26°± 5	20.°± 2	22°± 6
Day 26	77°± 4	5°±0	34°± 5	26°± 4	19°± 2	22°± 6

On day 0 (right after the sample preparation), all silver samples, that is TiNT-Ag-0, TiNT-Ag-5, TiNT-Ag-10, and TiNT-Ag-30 seconds reverse polarity surfaces, were hydrophilic with WCA of 7.4 ± 2.4°, 8.05 ± 2.2°, 8.95 ± 4.7°, and 6.25°± 1.518° respectively. A significant increase in WCA was observed for all groups after 24 hours (Day 1) compared to their respective wettability at Day 0, with WCA of 17.1 ± 2.6°, 29.9 ± 6.0°, 20.4 ± 4.9°, and 12.2± 3.676°, respectively, as seen in Table 1. As seen in Table 1, the TiNT group remained hydrophilic and had WCA values that were statistically different from all other groups. It was observed that the surface wettability was saturated to 26.7 ± 2.6° and 21.2 ± 1.8° for the 5 and 10 second reverse polarity samples, respectively, when monitored for a period of 26 days. However, an increase in WCA was observed for 0 sec reverse polarity samples to

33.6 ± 5.0° on day 26. Figure 6 shows the graphical representation of the WCA of the six different surfaces over 26 days.

Figure 6. Water Contact Angles for all Six Different Titanium Surfaces

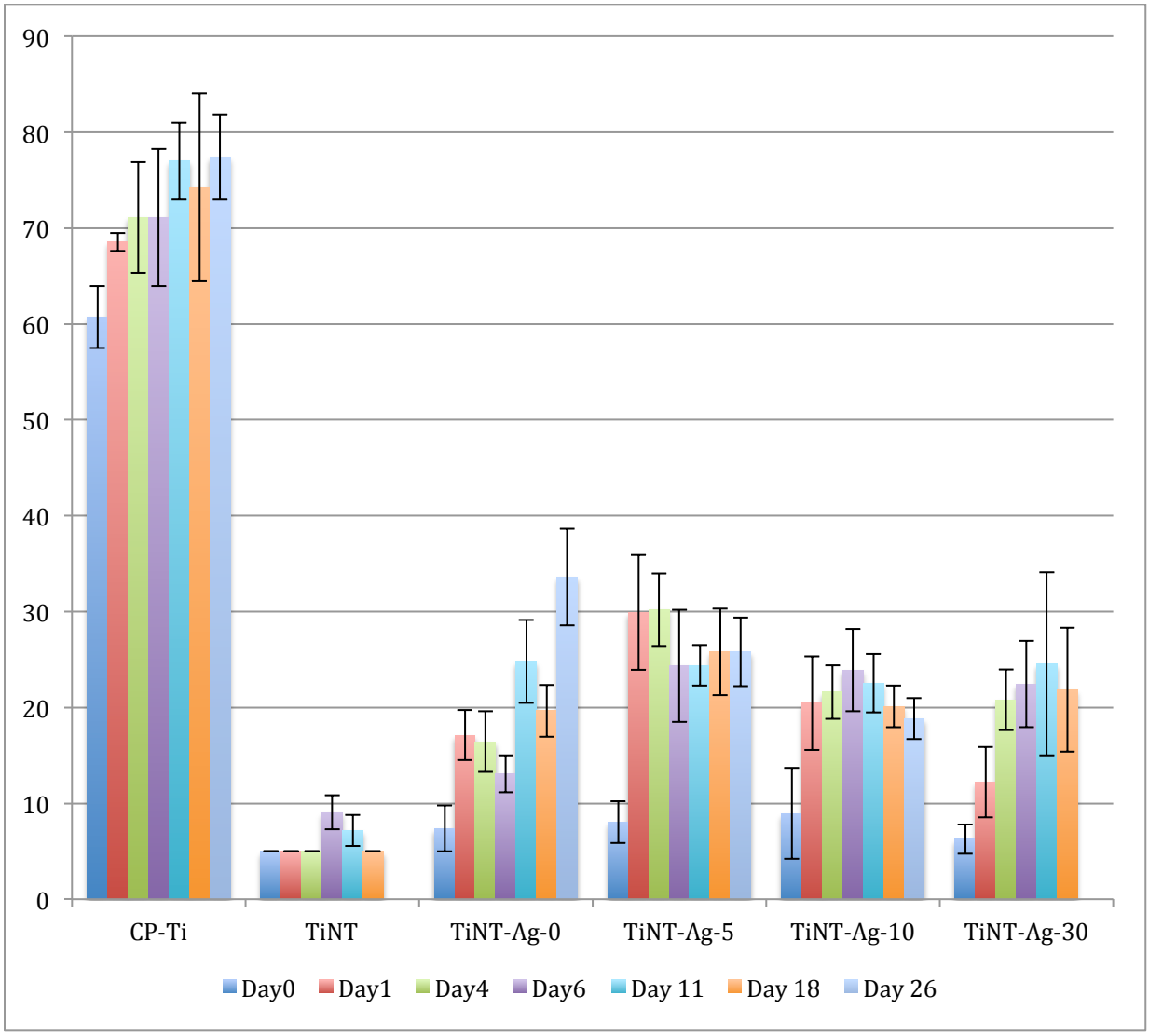

For reference: Hydrophilic surface WCA <90°, Super-hydrophilic surface WCA <5 °

4.1.4 White Light Interferometry

The surface roughness of the CP-Ti, TiNT, TiNT-Ag-0, TiNT-Ag-5, TiNT-Ag-10, and TiNT-Ag-30 samples were probed with white-light interferometry, and the R_a values recorded and zygo images captured for each surface type are seen in Figure 7.

Figure 7. White light interferometry readings for surface roughness. ***(A=CP-Ti, B=TiNT, C=TiNT-Ag-0, D=TiNT-Ag-5, E=TiNT-Ag-10, and F=TiNT-Ag-30)***

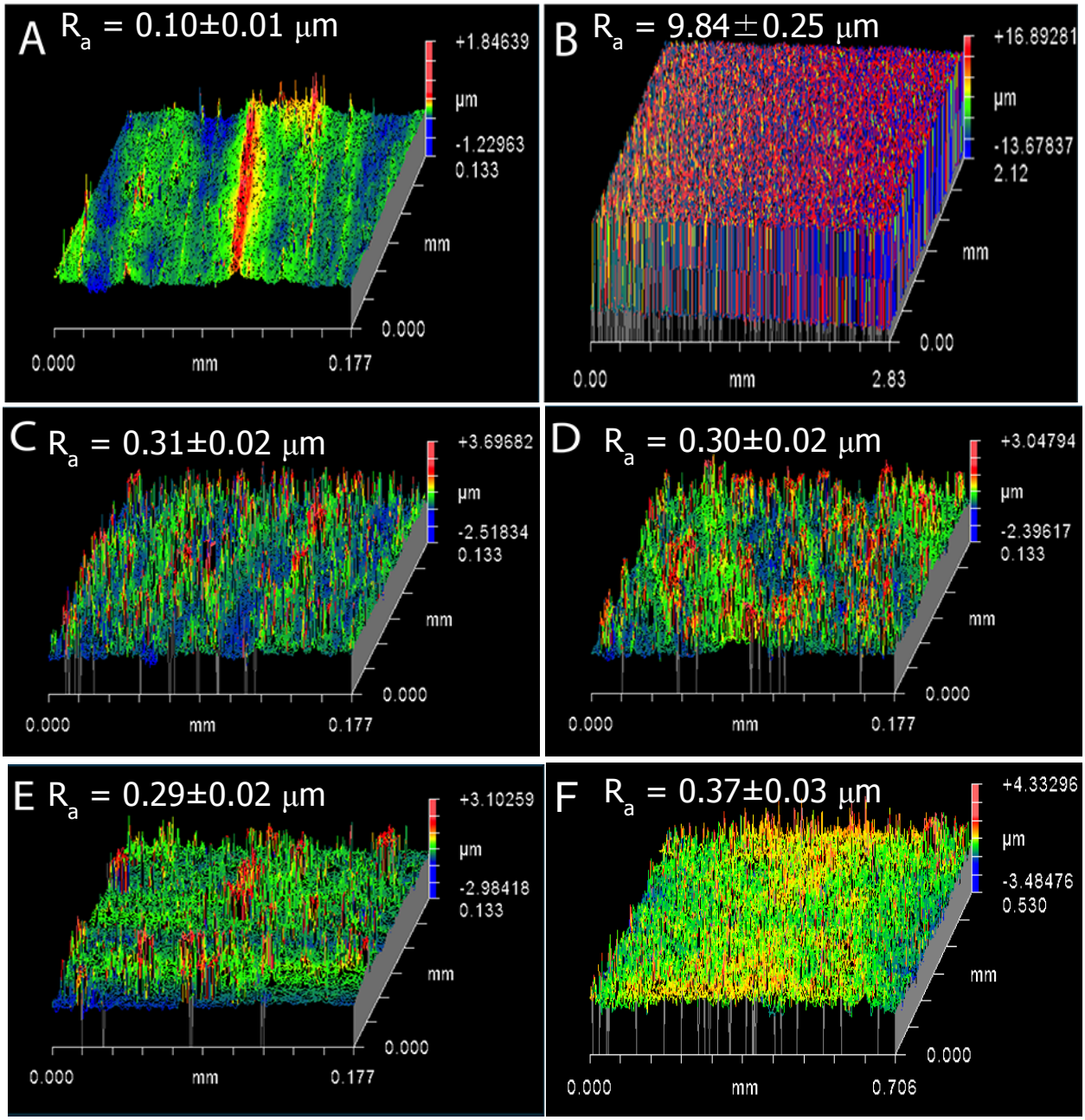

Table 2. White light interferometry readings for surface roughness.

Surface Group	Surface Roughness (R_a)
CP-Ti	0.10±0.01 μm
TiNT	9.84±0.25 μm
TiNT-Ag-0	0.31±0.02 μm
TiNT-Ag-5	0.30±0.02 μm
TiNT-Ag-10	0.29±0.02 μm
TiNT-Ag-30	0.37±0.03 μm

The surface roughness readings(R_a) from white light interferometry for the CP-Ti, TiNT, TiNT-Ag-0, TiNT-Ag-5, TiNT-Ag-10, and TiNT-Ag-30 groups were 0.10±0.01 μm, 9.84±0.25 μm, 0.31±0.02 μm, 0.30±0.02 μm, 0.29±0.02 μm, and 0.37±0.03 μm, respectively. The nanotubular surface without silver was almost 100x more rough than the CP-Ti. All the silver titania groups were about 3x as rough as CP-Ti, with the TiNT-Ag-30 having the greatest surface roughness value.

4.2 Bacterial Attachment

4.2.1 *In vitro* Attachment Assay

Preliminary *in vitro* of extra CP-Ti samples was conducted to determine the optimum incubation time for bacterial growth and optical density readings. CP-Ti was selected as a positive control. *P. gingivalis* was plated on CP-Ti, and OD_{550} readings were taken at 6-hr, 12-hr, and 24-hr time points, as seen in Table 3. 12-hr was then selected to be the optimum incubation time for OD_{550} readings (OD_{550}=0.2) within the sensitive range of the utilized spectrophotometer.

Table 3. Preliminary Data: Initial OD_{550} readings for *P. gingivalis* attachment to CP-Ti.

	6-hr	12-hr	24-hr
Sample #1	0.097	0.119	0.523
Sample #2	0.092	0.132	0.644
Sample #3	0.202	0.173	0.158
Sample #4	0.401	0.439	0.428
Average	0.198	0.216	0.438

In vitro attachment assay was performed after 12 hours of incubation of *P. gingivalis* on five surface types (CP-Ti, TiNT, TiNT-Ag-0, TiNT-Ag-5, TiNT-Ag-10, and TiNT-Ag-30). The crystal violet stain retained on the surface was washed off, and the solution was used to obtain OD_{550} readings for each of the 5 samples per surface group. The OD_{550}, average, standard deviation (SD), % reduction of bacterial attachment, and % bacterial attachment compared to TiNT are found in Table 4.

Table 4. Initial OD_{550} readings of extracted crystal violet stain for *P. gingivalis* attachment to titania surfaces. (EXPT#1)

	CP-Ti	TiNT	TiNT-Ag-0	TiNT-Ag-5	TiNT-Ag-10
Sample #1	0.345	4.57	0.633	0.474	0.602
Sample #2	0.392	6.21	0.567	0.647	0.557
Sample #3	0.291	3.72	0.731	0.493	0.704
Sample #4	0.31	5.52	0.634	0.555	0.562
Sample #5	0.324	3.60	0.603	0.527	0.681
SD	0.0387	1.13	0.0609	0.0678	0.0679
Average	0.332	4.72	0.634	0.539	0.621
Reduction (%)	/	0	86.6	88.6	86.9
% of the TiNT	7.04	100	13.4	11.4	13.1

The attachment assay readings (Table 4) were recalculated to account for the exact surface area of each individual sample (Table 5), and the optical density reanalyzed (Table 6). The four corners of each square sample were labeled as A, B, C, and D.

Table 5. Individual surface sample dimension measurements (mm) and calculated surface area (mm²). (EXPT #1)

Sample		CP-Ti	OD/S	TiNT	OD/S	TiNT-Ag-0	OD/S	TiNT-Ag-5	OD/S	TiNT-Ag-10	OD/S
#1	AB	5.87	0.0102	5.08	0.179	5.56	0.0217	5.35	0.0176	5.26	0.0222
	BC	5.96		5.13		5.15		5.07		5.11	
	CD	5.59		5.11		5.98		5.35		5.39	
	DA	5.88		4.92		4.98		5		5.08	
	AC	8.03		7.14		7.68		7.26		7.27	
	S	**33.9**		**25.6**		**29.2**		**26.9**		**27.1**	
#2	AB	5.44	0.0127	5.3	0.230	6.09	0.0171	5.38	0.0228	4.99	0.0211
	BC	5.44		5.14		5.66		5.43		5	
	CD	5.88		5.34		5.84		5.29		5.35	
	DA	5.54		5.08		5.48		5.21		5.21	
	AC	7.5		6.92		8.03		7.4		7.11	
	S	**30.8**		**27.0**		**33.2**		**28.4**		**26.4**	
#3	AB	5.26	0.0111	5.74	0.125	5.3	0.0248	5.35	0.0181	6.17	0.0223
	BC	4.99		5.24		5.34		5.09		5.1	
	CD	5.31		5.37		5.38		5.33		6.19	
	DA	4.9		5.48		5.72		5.1		5.12	
	AC	7.14		7.81		7.44		7.37		8.16	
	S	**26.1**		**29.7**		**29.5**		**27.2**		**31.6**	
#4	AB	5.28	0.00984	5.31	0.193	5.83	0.0206	5.05	0.0229	4.99	0.0201
	BC	5.98		5.38		5.37		5.08		5.56	
	CD	5.44		5.49		5.54		4.91		5.11	
	DA	5.81		5.23		5.48		4.96		5.54	
	AC	7.68		7.45		7.73		7		7.39	
	S	**31.5**		**28.6**		**30.8**		**25.0**		**28.0**	
#5	AB	5.28	0.0104	5.22	0.132	5.06	0.0230	5.44	0.0190	6	0.0228
	BC	5.7		5.47		5.33		4.96		5.06	
	CD	5.48		5.33		5.03		5.74		5.85	
	DA	5.59		5.4		5.07		5		5.01	
	AC	7.41		7.51		7.08		7.38		7.72	
	S	**31.1**		**28.7**		**26.2**		**27.8**		**28.8**	

Five types of surfaces were evaluated in the first bacterial attachment experiment. As shown in Table 6, the bacterial attachment based on the extracted bacterial solution crystal violet staining at OD_{550nm} readings were 0.0109±0.00114, 1.72±0.0437, 0.0214±0.00290, 0.0201±0.00259, and 0.0217±0.00111 for CP-Ti, TiNT, TiNT-Ag-0, TiNT-Ag-5, and TiNT-Ag-10, respectively. Using the TiNT as the standard (100%), the CP-Ti,

TiNT-Ag-0, TiNT-Ag-5, and TiNT-Ag-10 surfaces had bacterial attachment reduction of 93.7%, 87.5%, 88.3%, 86.9%, respectively. When compared to the TiNT group, reduction in attachment was observed at 93.0%, 86.6%, 88.6%, and 86.9% for the groups CP-Ti, TiNT-Ag-0, TiNT-Ag-5, and TiNT-Ag-10, respectively. For TiNT, the initial OD reading had an average of 3.61±0.43. Due to sensitivity of the spectrophotometer, the solution was diluted 10x, so the reading was within the sensitive reading range of OD<1.00 and then multiplied back 10x for accurate results. There seemed to be no difference among the different silver surface groups. The OD readings were greater for the silver groups compared to the CP-Ti, which indicates a potential increase in bacterial attachment on the nanotubular surface compared to smooth CP-Ti.

Table 6. *P. gingivalis* attachment based on spectrophotometer reading of extracted crystal violet stain from titania surfaces OD_{550} per mm^2. (EXPT #1)

OD/mm^2	CP-Ti	TiNT	TiNT-Ag-0	TiNT-Ag-5	TiNT-Ag-10
Sample #1	0.0103	0.179	0.0217	0.0176	0.0222
Sample #2	0.0127	0.230	0.0171	0.0228	0.0211
Sample #3	0.0111	0.125	0.0248	0.0181	0.0223
Sample #4	0.0098	0.193	0.0206	0.0229	0.0201
Sample #5	0.0104	0.132	0.0230	0.0190	0.0228
SD	1.1E-03	4.4E-02	2.9E-03	2.6E-03	1.1E-03
Average	0.0109	0.172	0.0214	0.0201	0.0217
Reduction (%)	93.7	0	87.6	88.3	87.4
% of the CNT	6.32	100	12.5	11.7	12.6

Figure 8 shows the actual *in vitro* attachment assay in a well plate with the crystal violet stain in the well (A) and after the stain was extracted (B). As seen in sub-picture A, the solution in the wells with TiNT has higher saturation of crystal violet and is visibly differentiable from all other surface groups. The silver surfaces had similar looking well

solutions with crystal violet. As seen in sub-picture B, there is some residual crystal violet stain on the TiNT surface group that was not washed off for the attachment assay.

Figure 8. CP-Ti, TiNT, TiNT-Ag surfaces with attached *P. gingivalis* after crystal violet stain. (A. picture showing the surfaces during attachment assay, B. picture showing what the surfaces look like after the assay and were left to air dry.)

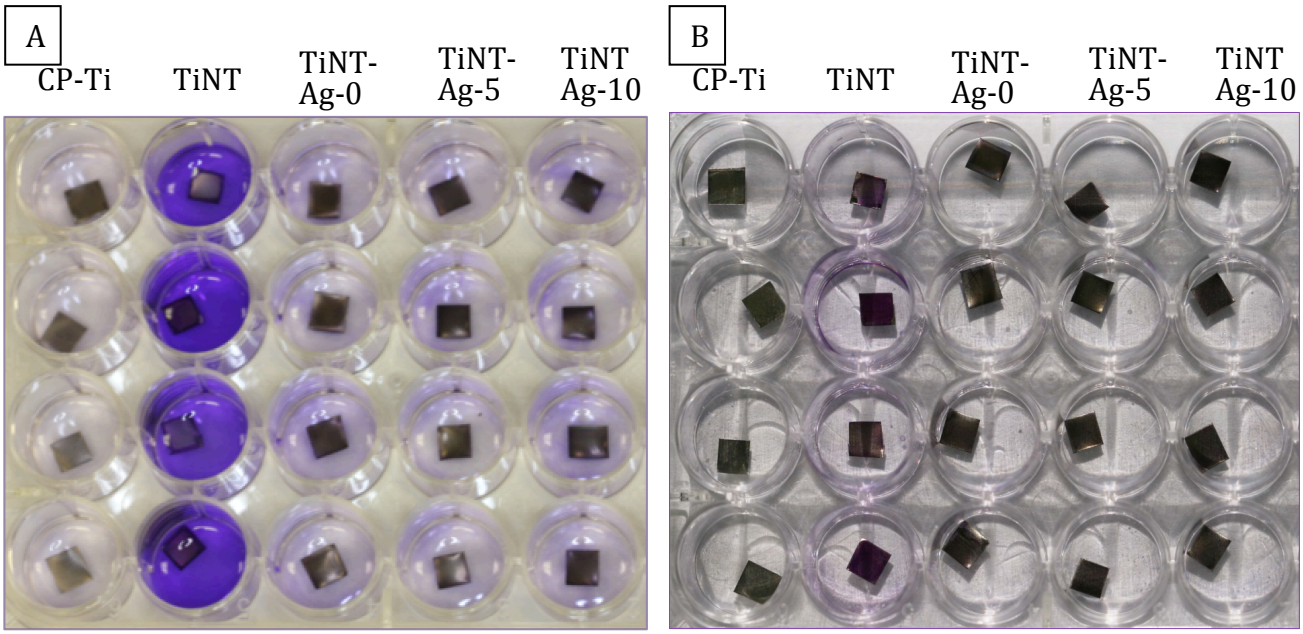

As seen in Figure 9, the OD_{550} readings for the five surface groups (CP-Ti, TiNT, TiNT-Ag-0, TiNT-Ag-5, and TiNT-Ag-10) were compared in a graphical representation.

Figure 9. Graph of *P. gingivalis* attachment on various titanium surfaces (EXPT #1)

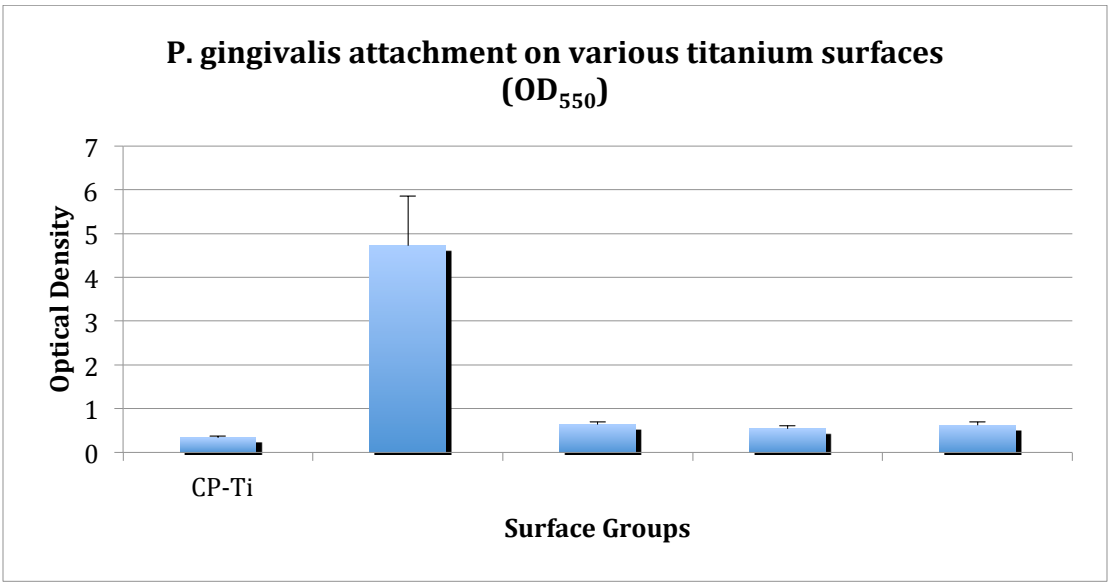

For live/dead staining of *P. gingivalis* on various surfaces, a second set of *in vitro* attachment assay was performed with identical test surface types and an additional TiNT-Ag-30 group to determine if more silver deposition on the surface would make a difference for bacterial attachment. For the second set of bacterial attachment assay, the 6 types of surfaces tested were CP-Ti, TiNT, TiNT-Ag-0, TiNT-Ag-5, TiNT-Ag-10, and TiNT-Ag-30.

P. gingivalis attachment as quantified by crystal violet stain was 0.225±0.0222, 5.95±0.323, 0.303±0.0380, 0.467±0.0735, 0.413±0.0445, 0.249±0.0582, for CP-Ti, TiNT, TiNT-Ag-0, TiNT-Ag-5, TiNT-Ag-10, and TiNT-Ag-30, respectively, as seen in Table 7.

Table 7. Initial OD_{550} readings of extracted crystal violet stain for *P. gingivalis* attachment to titania surfaces. (EXPT #2)

	CP-Ti	TNT	TNT-Ag-0	TNT-Ag-5	TNT-Ag-10	TNT-Ag-30
Growth Medium (Ctrl)	0.157	5.03	0.187	0.217	0.166	0.165
	0.157	4.06	0.171	0.183	0.167	0.17
	0.163	5.52	0.175	0.341	0.171	0.255
Average	0.159	4.87	0.178	0.247	0.168	0.197
STD	0.0035	0.74	0.0083	0.083	0.0027	0.051
Growth Medium with *P. g.* (*P. g.*)	0.241	5.56	0.301	0.486	0.445	0.331
	0.241	6.35	0.35	0.546	0.35	0.202
	0.194	5.93	0.257	0.369	0.444	0.214
Average	0.225	5.95	0.303	0.467	0.413	0.249
STD	0.0222	0.323	0.0380	0.0735	0.0445	0.0582
P. g. - Ctrl	0.0663	1.07	0.125	0.22	0.245	0.0523
% TNT	**6.16%**	**100%**	**11.6%**	**20.4%**	**22.8%**	**4.86%**
% reduction	93.8%	0	88.4%	79.6%	77.2%	95.1%

The dimensions of each individual sample were measured and listed in Table 7. The four corners of each square sample were labeled as A, B, C, and D. These measurements were taken to increase accuracy of the results by assessing if the surface area of each individual sample had significant variances that may have affected the optical density readings. Later statistical analyses confirmed that the samples were relatively uniform and

had similar trends for spectrophotometry readings, with and without accountability of each surface sample dimension. The attachment assay readings (Table 7) were recalculated to account for the exact size of each individual sample (Table 8), and the optical density reanalyzed (Table 9). There were three samples per surface type for this set of experiments. The "Growth Medium" control sample groups acted as a background for optical density readings.

Table 8. Individual surface sample dimension measurements(mm) and calculated surface area (mm²). (EXPT #2)

mm		Cp-Ti	TiNT	TiNT-Ag-0	TiNT-Ag-5	TiNT-Ag-10	TiNT-Ag-30
1	AB	5.26	4.79	5.54	5.56	4.68	5.01
	BC	5.11	4.85	5.29	5.25	5.11	4.49
	CD	5.16	4.93	5.5	5.42	4.93	5.2
	DA	4.94	4.96	5.46	5.38	5.08	4.63
	AC	7.06	6.73	7.64	7.67	6.9	6.6
	S	26.1	23.8	29.7	29.2	24.5	23.2
2	AB	5.82	4.77	4.99	5.85	5.27	5.16
	BC	5.53	4.81	5.23	5.09	5.31	4.53
	CD	5.68	5.1	4.84	5.72	5.23	5.24
	DA	5.29	4.66	5.27	4.91	5.22	4.45
	AC	7.87	6.71	7.06	7.42	7.26	6.66
	S	31.1	23.3	25.8	28.9	27.6	23.3
3	AB	4.88	5.31	5.61	5.82	5.79	4.84
	BC	4.95	4.93	5.19	4.9	5.26	4.71
	CD	4.92	5.27	5.59	5.69	5.66	4.82
	DA	4.97	4.82	4.96	5.04	5.36	4.67
	AC	6.77	7.12	7.52	7.27	7.69	6.47
	S	24.3	25.8	28.4	28.5	30.4	22.6

As seen in Table 9, The TiNT group has statistically significant higher bacterial attachment ($P<0.05$) compared to all other groups. Using the TiNT as the control (100%), the TiNT-Ag-0, TiNT-Ag-5, TiNT-Ag-10, and TiNT-Ag-30 surfaces had bacterial attachment reduction of 95.6%, 93.4%, 93.8%, and 95.6% respectively. The TiNT surface had greatest

recorded *P. gingivalis* attachment, and a 10x dilution of the crystal violet extract was used for OD_{550} reading.

Table 9. *P. gingivalis* attachment based on spectrophotometer reading of extracted crystal violet stain from titania surfaces OD_{550} per mm². (EXPT #2)

	CP-Ti	TiNT	TiNT-Ag-0	TiNT-Ag-5	TiNT-Ag-10	TiNT-Ag-30
OD/mm²	0.00922	0.234	0.0101	0.0167	0.0182	0.0143
	0.00775	0.272	0.0136	0.0189	0.0127	0.00867
	0.00800	0.230	0.00905	0.0130	0.0146	0.00948
SD	0.000786	0.0234	0.00236	0.00301	0.00280	0.00302
Average	0.00832	0.245	0.0109	0.0162	0.0152	0.0108
Reduction (%)	96.6	0	95.6	93.4	93.8	95.6
% of the CNT	3.40	100	4.45	6.61	6.20	4.41

As seen in Figure 10, the OD_{550} readings for the six surface groups (CP-Ti, TiNT, TiNT-Ag-0, TiNT-Ag-5, TiNT-Ag-10, and TiNT-Ag-30) were compared in a graphical representation.

Figure 10. Graph of *P. gingivalis* attachment on various titanium surfaces (EXPT:#2)

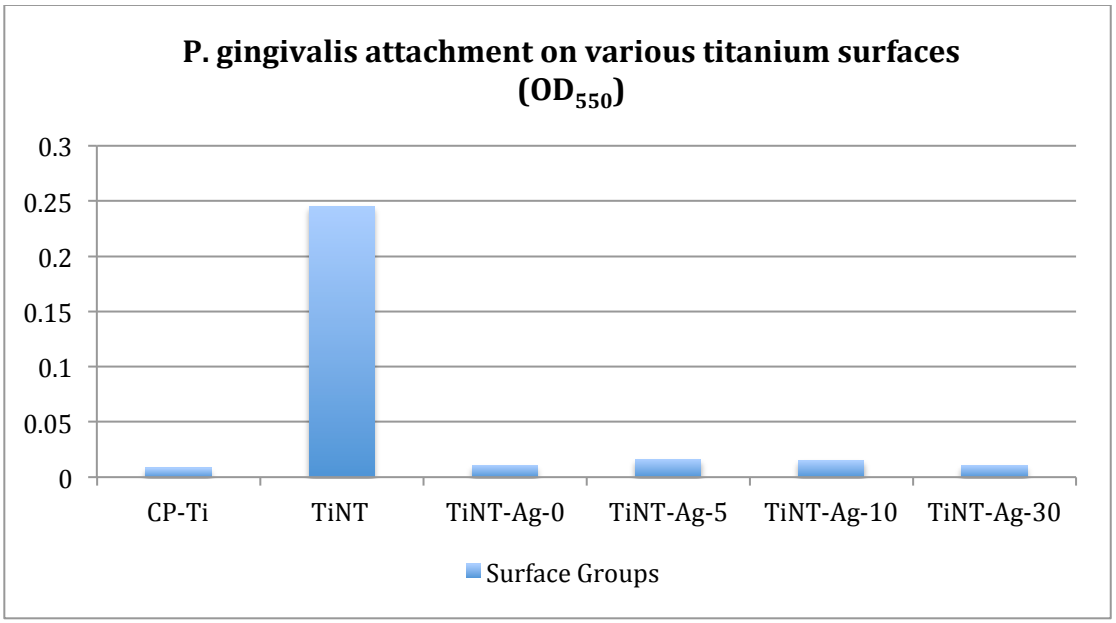

4.2.2 Live/Dead Stain

Figure 11. *P. gingivalis* viability: Live/Dead Stain *(Live, Dead, and Combined Stain: A=CP-Ti, B=TiNT, C=TiNT-Ag-0, D=TiNT-Ag-5, E=TiNT-Ag-10, and F=TiNT-Ag-30).*

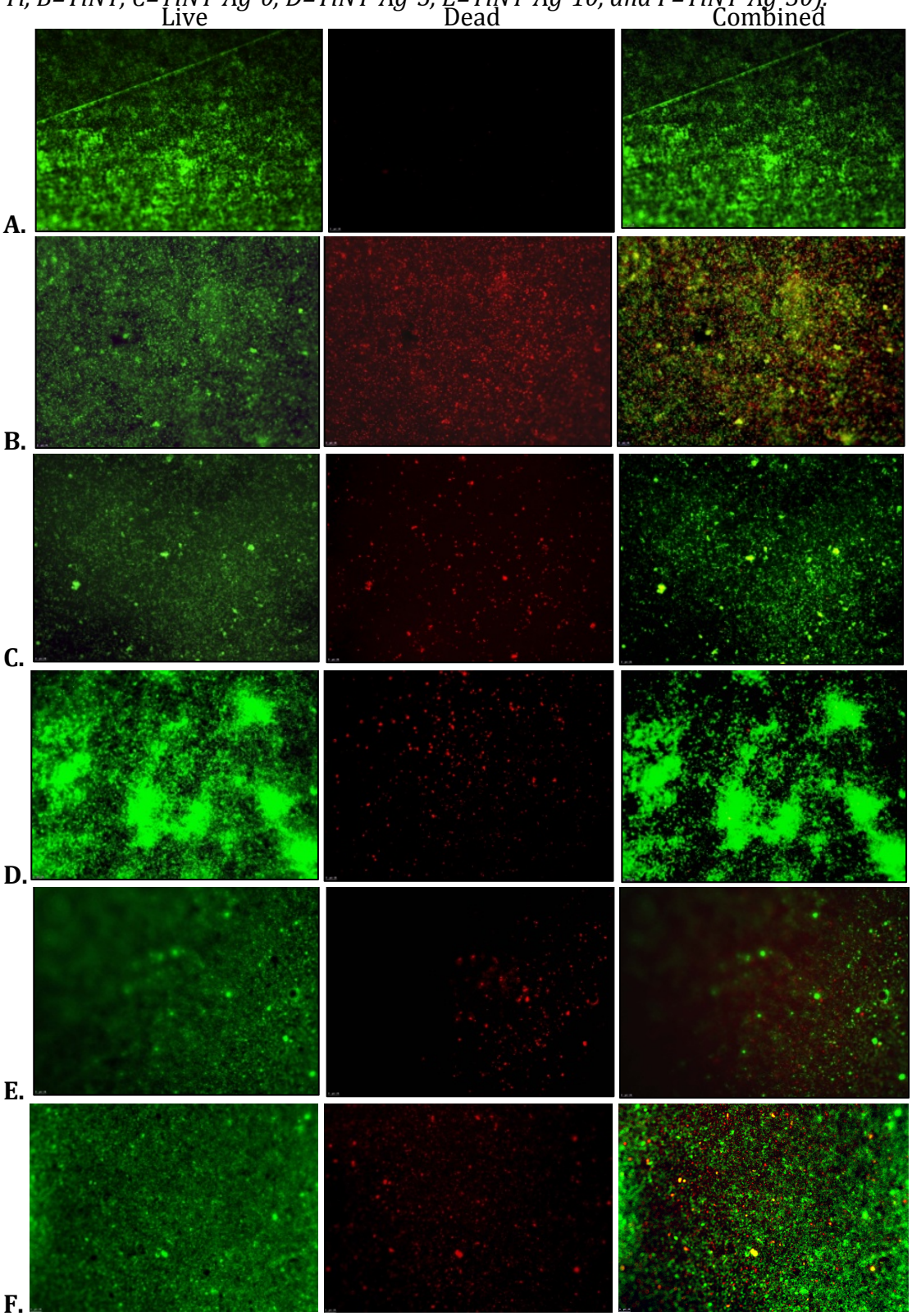

For Live/Dead stain analysis, a 40x live, dead, and combined stain views of each of the 6 surface groups (CP-Ti, TiNT, TiNT-Ag-0, TiNT-Ag-5, TiNT-Ag-10, and TiNT-Ag-30) were captured with the digital microscope camera and depicted in Figure 11.

Live and Dead stain analysis shows that TiNT and all silver surfaces had decreased live bacterial colonies compared to CP-Ti. All the CP-Ti and TiNT samples had live colonies, and CP-Ti had no observable dead colonies. The TiNT group had a qualitative death of ~2/3rds of the bacterial colonies on the surface. There were no observed differences among the silver groups, which have mostly cell death on the surfaces. The TiNT-Ag-5 group had an overexposed live count picture that may lead to a misleading read of increased live colonies. The live and dead stain results did not agree with the crystal violet staining results.

4.2.3 FESEM

Field emission scanning electron microscopy images were captured for the six different sample surfaces (CP-Ti, TiNT, TiNT-Ag-0, TINT-Ag-5, TiNT-Ag-10, and TiNT-Ag-30) following 12 hours of *P. gingivalis* bacterial attachment. In Figure 12, the three images presented for each of the surface groups were at 5,000X, 10,000X, and 20,000x magnifications. FESEM examination of the surfaces after *P. gingivalis* attachment showed the same uniform nanotubes as seen in the initial FESEM of the samples immediately after fabrication. *P. gingivalis* attachment was observed on all CP-Ti, TiNT, TiNT-Ag-0, and TiNT-Ag-4 surfaces. Very few *P. gingivalis* was seen attached to the TiNT-Ag-10 and TiNT-Ag-20 surfaces.

Figure 12. FESEM images for the surfaces after bacterial inoculation and incubation. *(A=CP-Ti, B=TiNT, C=TiNT-Ag-0, D=TiNT-Ag-5, E=TiNT-Ag-10, and F=TiNT-Ag-30).*

A. 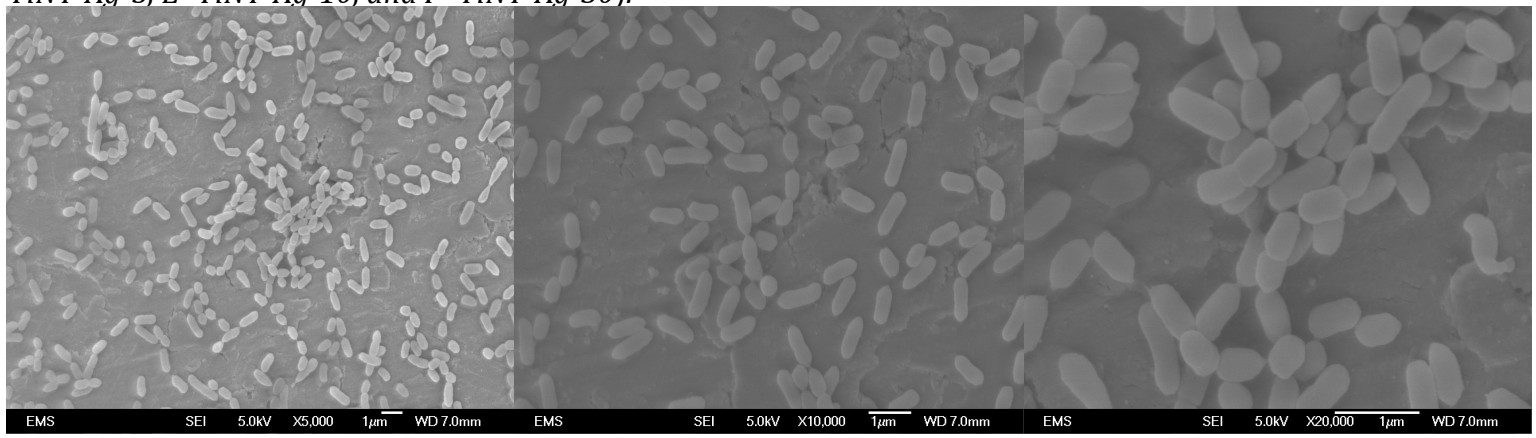

B.

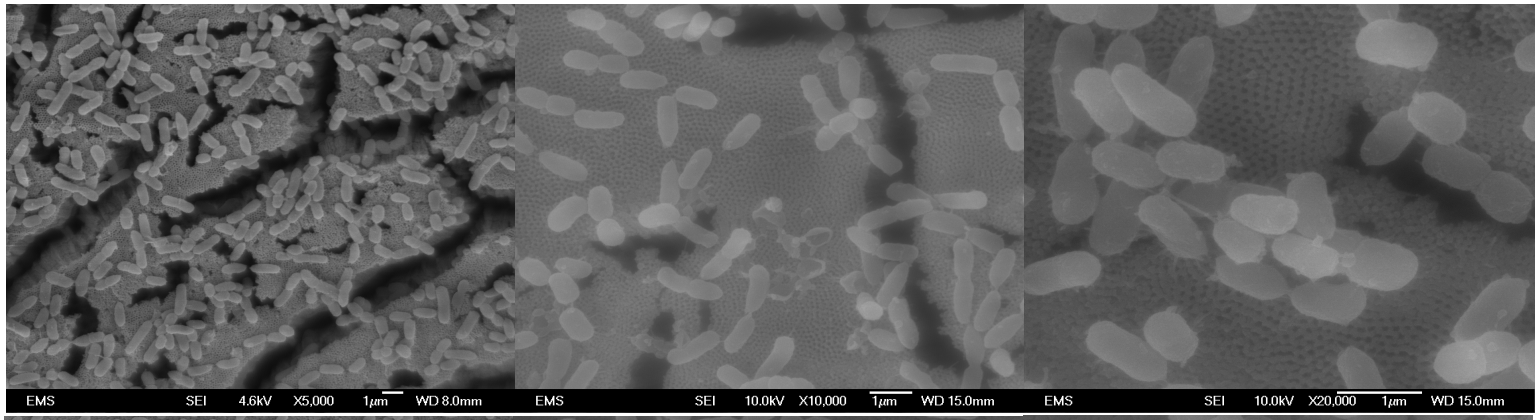
EMS SEI 4.6kV X5,000 1μm WD 8.0mm
EMS SEI 10.0kV X10,000 1μm WD 15.0mm
EMS SEI 10.0kV X20,000 1μm WD 15.0mm

C.

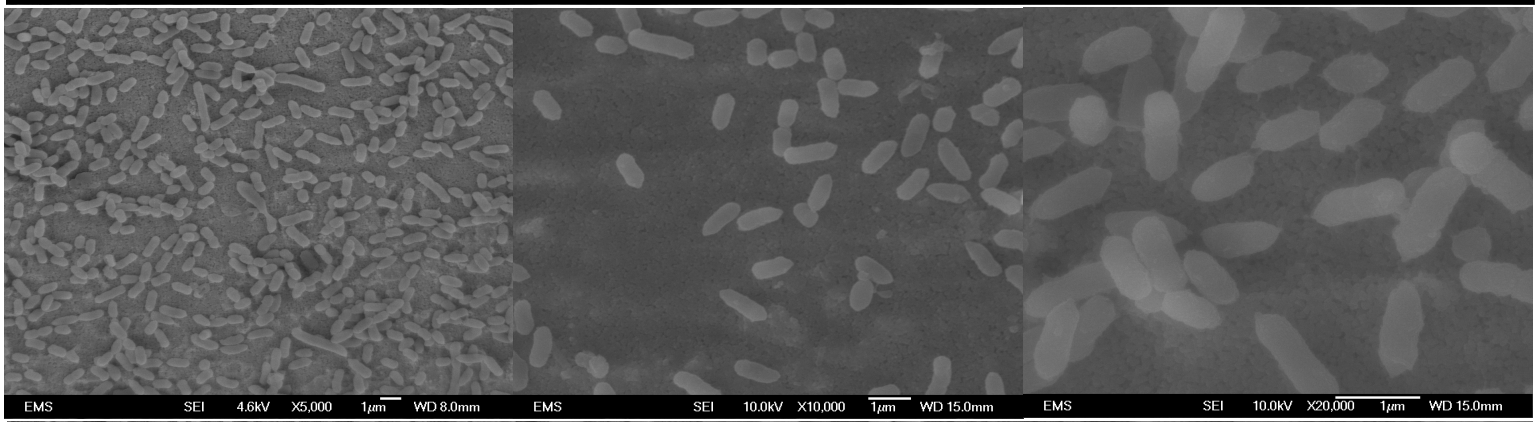
EMS SEI 4.6kV X5,000 1μm WD 8.0mm
EMS SEI 10.0kV X10,000 1μm WD 15.0mm
EMS SEI 10.0kV X20,000 1μm WD 15.0mm

D.

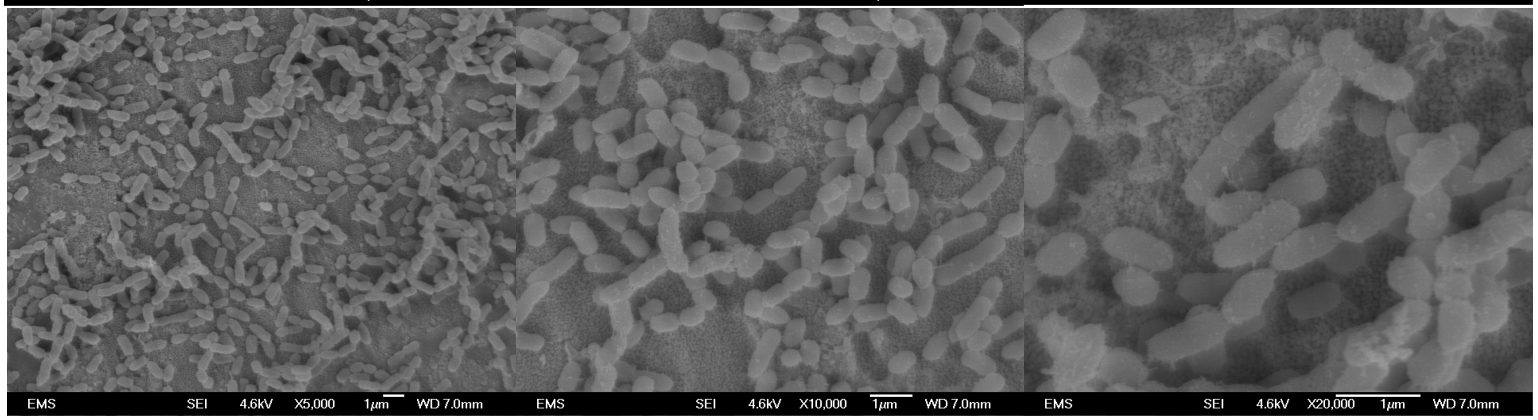
EMS SEI 4.6kV X5,000 1μm WD 7.0mm
EMS SEI 4.6kV X10,000 1μm WD 7.0mm
EMS SEI 4.6kV X20,000 1μm WD 7.0mm

E.

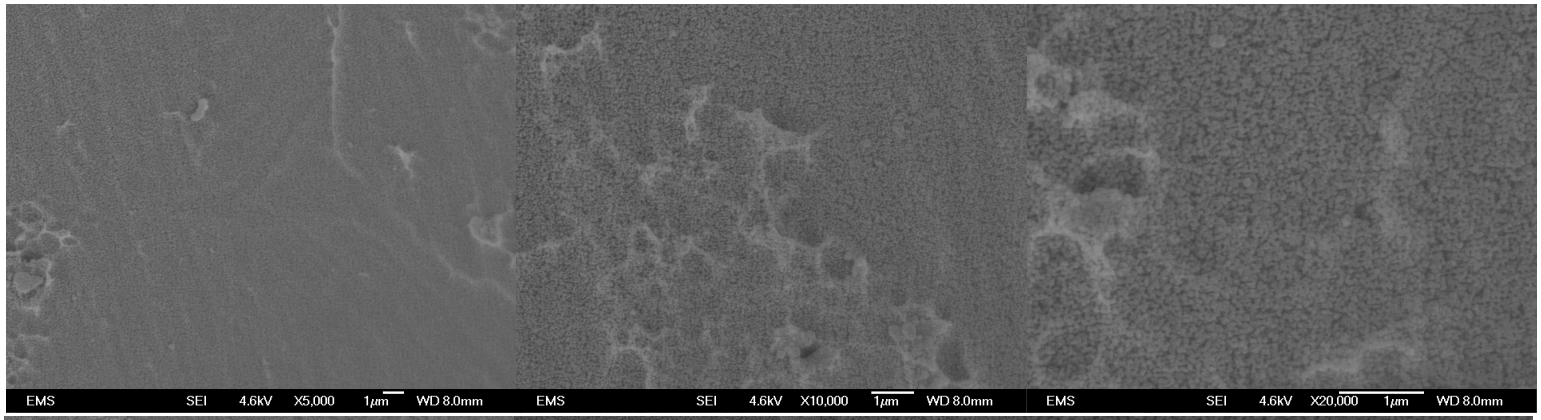
EMS SEI 4.6kV X5,000 1μm WD 8.0mm
EMS SEI 4.6kV X10,000 1μm WD 8.0mm
EMS SEI 4.6kV X20,000 1μm WD 8.0mm

F.

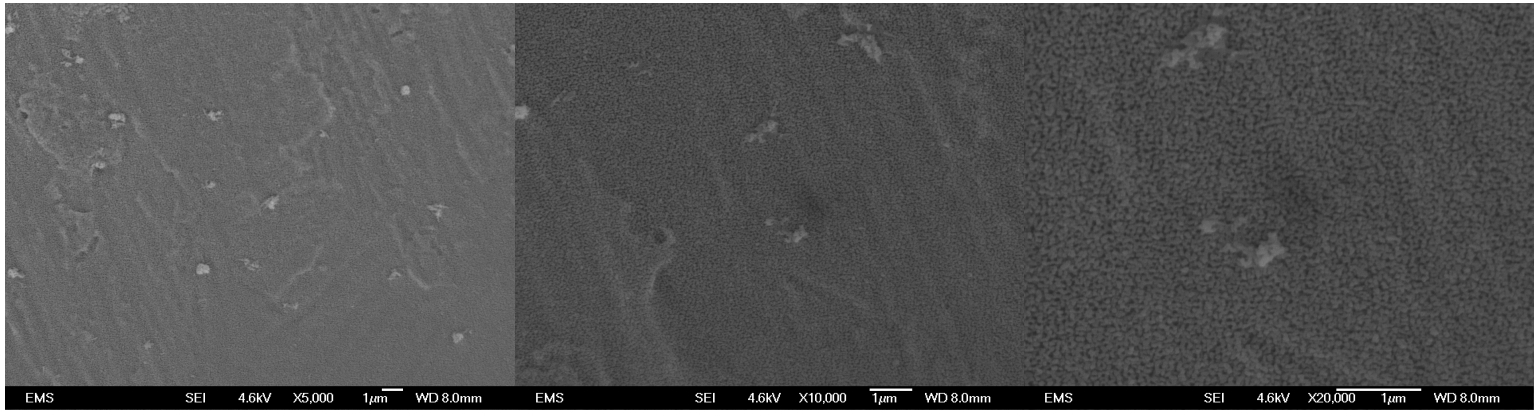
EMS SEI 4.6kV X5,000 1μm WD 8.0mm
EMS SEI 4.6kV X10,000 1μm WD 8.0mm
EMS SEI 4.6kV X20,000 1μm WD 8.0mm

5 DISCUSSION

5.1 Summary

Based on the results of this study, we are able to accept the hypotheses, the silver-embedded nanotubular titania surfaces significantly reduced (>87%) *P. gingivalis* attachment and biofilm formation ($p<0.05$). In summary, the incorporation of silver on the nanotubular surface seemed to have positive effects by modifying surface chemistry and reducing bacterial attachment and viability. Bacterial attachment was affected by surface roughness, surface free energy, and surface wettability. The results of this study are significant and will lead to further studies. We believe these silver-nanostructured surfaces could reduce bacterial attachment in vivo just as we found in vitro. Overall, this could mean less inflammation, improved ongoing tissue health, and reduced complications compared to what patients are currently experiencing. The novel dental implant surface could contribute to predictable long-term bone and soft tissue outcomes wanted by both patients and clinicians.

5.2 Surface Characterizations

5.2.1 FTIR

FTIR analysis was conducted for the CP-Ti, TiNT, TiNT-Ag-0, TiNT-Ag-5, TiNT-Ag-10, and TiNT-Ag-30 surface, as seen in Figure 4. Characteristic absorption peaks for H_2O and CO_2 were observed, and these peaks were expected as these two molecules were part of the FTIR system-purging chamber. Additionally, a broad peak was observed in all the samples in the range of 500 – 1100 cm^{-1} wavenumber, which was likely from the Ti-O, Ti-O-Ti, Ti-OH from titania nanotubes and Ag-O bond stretch from silver interaction with oxide of TiO_2.[22,85-90] Ag^+ and Ti^{4+} interaction with CO_2 has been shown to feature molecular bond vibration in the range of 2100 - 2200 cm^{-1}.[91] Similar FTIR spectra were observed for 5, 10, and 30 seconds reverse polarity samples, which indicated the similar surface composition of samples from all silver groups. This corroborated with the later described surface wettability and bactericidal data, where no significant difference among the three groups was observed. For 0 seconds reverse polarity, a broad absorption peak is observed between 2400-3400 cm^{-1}. This is likely from Ti-O-H molecular bond stretch that arise from the interaction of titania nanotubes with water, the C=O of carbon dioxide interacting with TiO_2 of titania nanotubes, the C-H absorption band from organic contamination from ambient environment, and/or remnant of 1,2-propanediol, which comes from the electrolyte of anodization.[85,90,92-96] TiNT seemed to be the most reactive surface in the FTIR chamber. This may indicate that the surface was not stable and reacted readily with other molecules and compounds. The hydrophobicity of this surface may be a manifestation of the reactivity.

5.2.2 FESEM & EDX

Field emission scanning electron microscopy and energy dispersive x-ray spectroscopy was completed for the six different sample surfaces (CP-Ti, TiNT, TiNT-Ag-0, TiNT-Ag-5, TiNT-Ag-10, and TiNT-Ag-30), as shown in Figure 5. All nanotubes samples yielded the same diameter nanotubes of ~ 80 – 100 nm from FESEM with clear pore openings. No difference in the external morphology between samples was observed likely due to the uniform preparation of all samples with the same conditions, except the length of time for silver deposition. EDX spectra proved the presence of silver along with other known elements including titanium, oxygen, carbon and fluoride for 0, 5, 10, and 30 seconds reverse polarity samples. The EDX also showed that non-silver samples had no silver contamination. This proved good execution of the protocol and no observed cross contamination in the system.

5.2.3 WCA & Wettability

Goniometric readings of the WCA for all the 6 surface types (CP-Ti, TiNT, TiNT-Ag-0, TiNT-Ag-5, TiNT-Ag-10, and TiNT-Ag-30) were taken on days 0, 1, 4, 6, 11,18, and 26, and recorded in Table 1. On day 0 (right after the sample preparation), all silver samples, that is TiNT-Ag-0, TiNT-Ag-5, TiNT-Ag-10, and TiNT-Ag-30 seconds reverse polarity surfaces, were hydrophilic with WCA of 7 ± 2°, 8 ± 2°, 9 ± 5°, and 6°± 2° respectively. Surface wettability depends surface energy, which is a function of surface composition and surface roughness. No significant difference in surface wettability among groups was observed, which was likely due to similar surface energy of titania nanotubes for these samples. After the samples were fabricated, the samples high surface energy resulted in hydroxyl group

formation, thereby making the surfaces hydrophilic. A significant increase in WCA was observed for all groups after 24 hours (Day 1) compared to their respective wettability at Day 0, with WCA of 17 ± 3°, 30. ± 6°, 20± 5°, and 12± 4°, respectively, as seen in Table 1. The increase in WCA was likely due to 1) loss of hydroxyl groups from the surface making samples less hydrophilic or 2) possible organic contamination from the ambient environment due to the reactivity of high energy surface with low volatile organics in environment.[103] Because the duration and voltage for anodization was the same for all four silver groups, the surface roughness of the samples may not be a leading factor affecting the surface wettability, as samples from all groups have the same surface roughness, but different WCA values.

After 6 days, all groups except for the TiNT-Ag-0 reached their relative maximum WCA and plateaued for the rest of the 26 days. As seen in Table 1, the TiNT group remained hydrophilic and had WCA values that were statistically different from all other groups. It was observed that the surface wettability was saturated to 27± 3° and 21 ± 2° for the 5 and 10 second reverse polarity samples, respectively, when monitored for a period of 26 days. No statistical difference was observed among the silver embedded groups. The TiNT-Ag-0 surface group seemed to be have inconsistent readings overall over the 26 days, which may indicate that this surface was unstable compared to the other surface groups. From the WCA data, it was concluded that all samples became more hydrophobic the day after their preparation, which may be due to the loss of hydroxyl groups from the surface or the possible contamination from the ambient environment. The hydroxyl groups are electrochemically attracted to water and ions and provide hydrophilicity for surfaces.

The water contact angle measurements for this study were in agreement with other published literature on water contact angles values on polished commercially pure titanium, (61°± 3 vs. 58.5°).[26] Unlike Mekayarajjananonth and Winkler's study, the rougher surfaces in this study compared to CP-Ti, had smaller water contact angles than the treated, rougher surfaces in their study. This could be explained by increased surface area and surface free energy that renders the rough surface more hydrophilic than CP-Ti. The water contacts angles measured were within a full degree. The accuracy of the wettability analysis could be improved with an improved goniometric device with less measurement error.

5.2.4 White Light Interferometry.

As seen in Table 2, the surface roughness readings (R_a) from white light interferometry for the CP-Ti, TiNT, TiNT-Ag-0, TiNT-Ag-5, TiNT-Ag-10, and TiNT-Ag-30 surfaces were 0.10±0.01 μm, 9.84±0.25 μm, 0.31±0.02 μm, 0.30±0.02 μm, 0.29±0.02 μm, and 0.37±0.03 μm, respectively. The nanotubular surface without silver was almost 100x more rough than the CP-Ti. All the silver titania groups had mean R_a=0.3-04μm, which was about 3x as rough as CP-Ti. The TiNT-Ag-30 surface had the greatest surface roughness value. Higher surface roughness increased bacterial attachment and consequent biofilm formation. Also, better organization of a lattice structure, as in the case of uniform nanotubular surface, increases surface energy and wettability and can be further potentiated by surface roughness.

According to Albrektsson and Wennerberg's classification, the CP-Ti surface is considered smooth, the TiNT surface is a rough surface, and all of the TiNT-Ag groups are minimally rough, which is most similar to most commercially available dental implants.[27] This shows that titanium nanotubular surfaces alone with no silver may be too rough of a surface and more conducive to bacterial attachment due to high surface roughness (Wenzel's Law). When the surface was tempered with silver, the-benefit of a more desirable surface roughness for improved wettability was achieved as well.-When silver was added to the nanotubular surface, the FTIR readings were much more consistent and stable. Silver may improve not only the surface roughness but also maintain the surface energy and stability of the titania nanotubular surface.

5.3 *P. gingivalis* Biofilm Attachment

5.3.1 *In vitro* Attachment Assay via Crystal Violet Staining

In the first bacterial attachment experiment, significantly higher bacterial attachment ($P<0.05$) was observed in TiNT compared to other groups. Using TiNT as the comparison (100%), the CP-Ti, TiNT-Ag-0, TiNT-Ag-5, and TiNT-Ag-10 surfaces had bacterial attachment reduction of 93.0%, 87.6%, 88.3%, 87.4%, respectively. The results showed that the silver deposited samples had less bacterial attachment than nanotubular titania surfaces without silver. Thus, silver inhibited bacterial growth and decreased biofilm formation. The bacterial attachment may be dependent on the surface morphology and characteristics in addition to the influence of silver. All the silver samples became more hydrophobic over time based on water contact angle data. There seemed to be no difference among the various silver groups.

The TiNT group has the most saturated violet stain compared to all other groups. After the experiment was done and the samples left out to dry, residual violet stain was observed on the samples, especially the TiNT group, as seen in Figure 8. This may indicate that the stain was trapped in the surface possibly due to the surface architecture of the nanotubes. If all of the crystal violet stain were extracted from the surface for OD_{550} reading, then the bacterial reduction (%) may have been greater than the current readings. However, as previously mentioned, *P. gingivalis* is not an initial colonizer of an intraoral biofilm and may easily be detached from a surface during the wash steps of the protocol. Thus, the OD_{550} may be more of a representation of crystal violet bond to the surface and not crystal violet bond to *P. gingivalis*. The crystal violet stain was employed in this study,

as it is one of the standard *in vitro* assay methods to assess bacterial attachment in pilot studies. Future tests with more direct measurements such as confocal microscopy are recommended to either confirm or better clarify the influence of the nanotubular surface on bacterial attachment and biofilm formation.

For live/dead stain, a second set of *in vitro* attachment assay was performed with identical test surface types and an additional TiNT-Ag-30 group. Because there was no statistically significant difference in reduction of bacterial attachment among the silver groups in the first experiment, the TiNT-Ag-30 group was added to see if more silver deposition on the surface would make a difference in bacterial attachment.

For the second set of crystal violet staining of *P. gingivalis*, 6 types of surfaces were tested: CP-Ti, TiNT, TiNT-Ag-0, TiNT-Ag-5, TiNT-Ag-10, and TiNT-Ag-30. The spectrophotometer average optical density readings were 0.225±0.0222, 5.95±0.323, 0.303±0.0380, 0.467±0.0735, 0.413±0.0445, 0.249±0.0582, for CP-Ti, TiNT, TiNT-Ag-0, TiNT-Ag-5, TiNT-Ag-10, and TiNT-Ag-30, respectively, as seen in Table 7. The TiNT group has statistically significant higher bacterial attachment ($P<0.05$)–compared to all other groups, which is likely due to the higher surface energy from the TiNT nanotubular surface that allowed for the wettability and adhesion of surface molecules by *P. gingivalis*. Using the TiNT as the standard (100%), the TiNT-Ag-0, TiNT-Ag-5, TiNT-Ag-10, and TiNT-Ag-30 surfaces had bacterial attachment reduction of 95.6%, 93.4%, 93.8%, and 95.6% respectively. The silver deposited samples had less bacterial attachment than non-silver nanotubular titania surface. However, the OD_{550} readings were less sensitive than the first

experiment, so the first experiment had more valid results. The data was in general agreement with the first set of experiment. The TiNT-Ag-30 surface had a significant increase in bacterial reduction compared to the other silver groups, but this difference was not statistically significant.

5.3.2 Live/Dead Stain

Live and Dead stain analysis showed that TiNT and all silver surfaces had decreased live bacterial colonies compared to CP-Ti. All the CP-Ti and TiNT samples had live colonies, and CP-Ti had no observable dead colonies. The TiNT group had a qualitative death of ~2/3rds of the bacterial colonies on the surface. There were no observed significant differences among the silver groups, which had mostly cell death on the surfaces. Live and Dead stain analysis is a very technique sensitive procedure and has the least reliable results of the performed bacterial *in vitro* assays.

5.3.3 FESEM

The FESEM images of all six different sample surfaces (CP-Ti, TiNT, TiNT-Ag-0, TINT-Ag-5, TiNT-Ag-10, and TiNT-Ag-30) following 12 hours of *P. gingivalis* bacterial attachment are seen in Figure 12. The FESEM of the samples post bacterial attachment showed the same uniform nanotubes as seen in the initial FESEM of the samples immediately after fabrication. This may indicate the surface morphology was stable over time. The magnifications were 5000x, 10,000x, and 20,000X. *P. gingivalis* attachment was observed on all CP-Ti, TiNT, TiNT-Ag-0, and TiNT-Ag-4 surfaces. Very few *P. gingivalis* was seen attached to the TiNT-Ag-10 and TiNT-Ag-20 surfaces. This may indicate that both

groups already have reached the minimum inhibitory concentration of silver, although there was still bacterial attachment based on the *in vitro* attachment assay. The difference in results between the two different assays stem from the different methodologies and the strengths and weaknesses of each method, which is discussed in the following section.

5.3.4 Summary of *P. gingivalis* Biofilm Attachment

The samples fabricated were flat surfaces, which provided ease of fabrication and handling. During the bacterial attachment assay, it was noted that under the microscope, the surfaces were observed to be slightly curved along the edges and were imperfect squares. Therefore, the exact dimensions of every sample were measured. For future experiments, the characteristics and behavior of the surface may be changed when it is prepared in the screw form to match the standard anatomy of endosteal implants. Bacterial and cellular attachment may become more complicated, as the biofilm around the titanium surface will need to grow in three dimensions instead of strictly laterally.

The exact *P. gingivalis* attachment mechanism is not known, but the pathogen is considered a late colonizer that relies on interaction with the preexisting biofilm's bacteria and extracellular matrix receptors to form a strong, permanent bond to a surface.[65] Otherwise, *P. gingivalis* fimbrae and adhesins alone are considered relatively weak bonds, and *P. gingivalis* had been observed in previous studies to attach to dental material surfaces less compared to other periodontal pathogen.[67, 70, 72] Perhaps due to this behavior, the bacterial attachment results found with crystal violet stain underreported the amount of bacterial attachment, as the *P. gingivalis* may have easily been washed off during the assay

steps. As a Gram-negative bacterium, *P. gingivalis* has an outer negatively charged LPS membrane protecting an inner membrane full of peptidoglycan, the main component of Gram-positive bacteria. Silver ions (Ag^+) are positively charged and may therefore, from on an electrochemical standpoint, be more attracted to *P. gingivalis* from complementing charge attraction. Perhaps another kind of stain assay would be more appropriate for the bacteria as well.

The *in vitro* attachment assay, live/dead stain, and FESEM had some conflicting results on the presence and attachment of bacteria. From the FESEM post bacterial inoculation, the titanium nanotubular group (TiNT) had more bacteria than the commercially pure titanium control (CP-Ti). In fact, TiNT was observed to have the most bacteria under FESEM analysis. The TiNT-Ag-0 and TiNT-Ag-5 groups were comparable. The TiNT-Ag-10 and TiNT-Ag-30 groups both had no visible bacteria. However, based on the crystal violet assay, there were still bacteria attached on the TiNT-Ag-10 and TiNT-Ag-30 surface groups. Furthermore, the live/dead stain showed bacterial cell death on about 2/3rds of the TiNT surface, which based on FESEM and crystal violet stain showed the highest bacterial attachment. The greatest number of bacterial colonies was observed on the CP-Ti control for the live/dead stain. Based on the live/dead stain, all the silver groups (TiNT-Ag-0, TiNT-Ag-5, TiNT-Ag-10, and TiNT-Ag-30) had significantly more cell death than the CP-Ti and TiNT, but had comparable results among the silver groups. This may be a limitation of the live/dead stain process itself in that the bacteria may be dead or damaged by the time the silver groups were tested. The live/dead stain analysis itself is time and technique sensitive. Perhaps the resolution was not optimal either, so the results

were not as clear. Also, the live/dead stain is a qualitative test that is not as powerful and reliable of a test as the crystal violet stain. The FESEM is the weakest and most qualitative test of all three *in vitro* attachment analyses. The *in vitro* attachment assay is the strongest of the three tests. Therefore, it was concluded that *P. gingivalis* attachment was highest on TiNT and experienced statistically significant decrease (>87%) in attachment on all silver-embedded titania nanotubular surfaces ($p<0.05$).

5.4 Integration of All Results

Table 10. Comprehensive Summary of All Results

Comprehensive Summary of All Results						
Surface Group	CP-Ti	TiNT	TiNT-Ag-0	TiNT-Ag-5	TiNT-Ag-10	TiNT-Ag-30
FTIR	H_2O, NH^{4+}, Ti-OH, TiO-NH_3; TiO, Ti-O-Ti, Ti-OH	H_2O; C-H; CO_2; NH^{4+}, Ti-OH, TiO-NH_3; TiO, Ti-O-Ti, Ti-OH	H_2O; C-H; CO_2; NH^{4+}, Ti-OH, TiO-NH_3; TiO, Ti-O-Ti, Ti-OH	H_2O, NH^{4+}, Ti-OH, TiO-NH_3; TiO, Ti-O-Ti, Ti-OH	H_2O, NH^{4+}, Ti-OH, TiO-NH_3; TiO, Ti-O-Ti, Ti-OH	H_2O, NH^{4+}, Ti-OH, TiO-NH_3; TiO, Ti-O-Ti, Ti-OH
FESEM	smooth	uniform, 80-100nm diameter	uniform, 80-100nm diameter	uniform, 80-100nm diameter	uniform, 80-100nm diameter	uniform, 80-100nm diameter
WCA (day 1)	61°± 3	5°± 0	7°± 2	8°± 2	9.°± 5	6°± 2
WCA (Day 26)	77°± 5	5°± 0	34°± 5	26°± 4	19°± 2	22°± 7
WLI (μm)	0.10±0.01	9.84±0.25	0.31±0.02	0.30±0.02	0.29±0.02	0.37±0.03
% Reduction of Attachment (EXPT#1)	93.7	0	87.6	88.3	87.4	N/A
% Reduction of Attachment (EXPT#2)	96.6	0	95.6	93.4	93.8	95.6
Live/Dead Stain	live	live (2/3rd dead)	dead	dead	dead	dead
FESEM (bacteria present?)	+	+	+	+	-	-

For better visual comparison, the summary of all of the results was compiled in Table 10 for comparison of surface characterizations and bacterial attachment. For all of the surface characterizations, the data were mostly consistent with each other. The technique was sound, and little to no contamination was perceived. The most notable

difference was that TiNT with no silver had the most sensitive reading under FTIR. Again, the authors of this study speculate that the surface has higher reactivity and free energy and reacted strongly with the ambient environment to form more defined C-H, CO_2, H_20, NH^{4+}, Ti-OH, and TiO-NH_3 bonds than all other surfaces. The CP-Ti was a very stable surface and had relatively little readings from FTIR. TiNT's surface reactivity and high surface area, plus the highest R_a value out of all the surfaces, could explain why the bacteria attached the most to this surface. Perhaps the crystal violet bound the most to this rough surface as well, which can overinflate the *in vitro* assay results, and the OD_{550} may represent a combination of the crystal violet bond to the surface and to *P. gingivalis* on the surface of TiNT. Although all nanotubular groups were more hydrophilic than the CP-Ti control, the TiNT group was the only group that could be considered super-hydrophilic. Thus, the surface energy, surface stability, high wettability and surface roughness of the titania nanotubular surfaces may be the main promoters of biological cell attachment to these surfaces.

For the bacterial assay, the conflicting results were observed between the FESEM and crystal violet stain results of the silver group. While the FESEM showed no bacterial attachment on the TiNT-Ag-10 and TiNT-Ag-20 groups, the crystal violet staining and live/dead staining still had attachment observed and visible colonies. Again, the crystal violet assay is the strongest and most reliable of the three types of bacterial assessment, so we could not conclude that any of the titania nanotubular surface groups were bactericidal. However, the incorporation of silver into the titanium nanotubular surface statistically significantly lowered the attachment of *P. gingivalis* ($P<0.05$).

The FTIR and TEM data confirmed that silver was embedded in the implant surface and had both silver oxide and silver ions. Silver oxide is a relatively stable compound used in some batteries as well as other antimicrobial applications.[74] The silver ion may increase the likelihood of corrosion and unfavorable effects on the peri-implant tissues such as porcelain greening of prosthetic components or staining of the hard and soft tissue much like an amalgam tattoo. While the surface may cause few biological complications, the silver ions may compromise the final esthetic result. It may be possible that there were electrolytes remaining from the solution after the sterilization protocol, which may provide extra silver ions to react with the bacteria. The possibility of this contamination is considered to be small due to the EDX and FTIR readings revealing the absence of the known electrolytes from the preparation solutions.

The silver may act through antimicrobial mechanisms within the bacteria or simply prevent bacterial attachment by making a surface electrochemically unfavorable and difficult for bacteria attachment, even though the silver embedded nanotubular surfaces were all at least 3x as rough as CP-Ti, and by Wenzel's law, should protect bacteria from shear forces and promote maturation of bacteria attachment bonds. Compared to TiNT though, the silver surfaces had lowered surface roughness, which could explain the decreased bacterial attachment.

The incorporation of silver also seemed to change the surface characteristics of the samples for unforeseen improved biological response in addition to the proposed antimicrobial enhancement. Most of silver embedded nanotubular surfaces (TiNT-Ag-5,

TiNT-Ag-10, and TiNT-Ag-30) were able to reach and maintain a relative maximum water contact angle by Day 6. In fact, as the amount of silver incorporated into the titanium nanotubes were increased, the water contact angle lowered. Thus, silver increased the surfaces hydrophilicity and wettability, except for TiNT-Ag-0, and higher amounts of silver deposition would be recommended in the future. Also, the silver changed the titanium nanotubular surface from rough to moderately rough (9.84±0.25 μm vs 0.32±0.02 μm) surface, which clinically performs better with relatively few peri-implant complications. If the TiNT-Ag surfaces have high surface stability, then perhaps the antimicrobial properties of this surface could be potentiated over a long-term period as well. Overall, the combination of surface nanotube formation and silver incorporation transformed and improved the surface characteristics of the titanium surface and also inhibited *in vivo P. gingivalis* attachment and biofilm formation.

5.5 Weakness and Limitations of the Study

The preparation of the foil specimens post anodization may have damaged, changed, or contaminated the surfaces, especially along the edges of the specimens. At 0.25mm, the foils were thin and relatively pliable and may have lost surface flatness at the macro level along the edges where the specimens were cut into 5mm x 5mm pieces for subsequent experimentation. The possibility of contamination was decreased by the use of sterilized instruments and subsequent ethylene dioxide gas sterilization of the foil specimens.

Titanium discs of greater thickness would have been another viable option for specimen preparation. The surfaces would potentially have more rigidity and surface stability. If titanium disc specimens were used, the collected analysis for FESEM, EDX, and FTIR would not have been different from the results in this study, but WLI and water contact angles may be slightly different due to a larger, flatter surface. The difficulty of creating titanium discs would be needing to anodize each sample separately and potentially have different amounts of silver embedded within the surface for each surface group type. The loss of uniformity and standardization of anodization protocol may slightly affect the intensity of the surface characterizations collected, but the absorption peaks and characteristic findings would likely still be the same. Otherwise, anodization of a greater surface area disc and consequent cutting of the discs into desired dimensions would still introduce the potential for specimen damage and contamination, especially along the edges of the surface specimens.

The screw form of a dental implant may create a more fragile surface with greater surface area due to the geometry of nanotubes along a curved surface. The hydrophilicity and surface roughness may be increased on a screw form implant relative to the flat specimens, which may lead to improved biological cell attachment and osseointegration. The stability and aging (i.e. corrosion and wear) of the surface may be decreased on the curved screw surface from due to the handling of the implant during surgery. Further tests on surface handling and aging of the novel silver nanotubular surface are necessary to better understand the influence of silver nanotubes on a titanium dental implant surface.

Other limitations of this study relate to the fact that the *in vitro* environment that the study was conducted in did not reflect a realistic intraoral biofilm environment. Adhesion association with pellicle and plaque could change the results. The study assessed the surfaces' antimicrobial properties with only one bacterial species without the presence of a mature intraoral biofilm. Future studies could evaluate the adhesion of biofilm molecules on the surfaces and how those molecules affect bacterial adhesion. The biofilm molecules could facilitate bacterial adhesion and reduce the antimicrobial potential of the novel silver surface.

The study could also have improved study design in the selection of a reference surface. The reference surface used was commercially pure titanium. However in the clinical word, the standard is an appropriately roughened or machined Ti surface. A more telling control group with an appropriate standard surface roughness (R_A=1.0-2.0um) and surface treatment would more effectively compare the influence of nanotubes against the

standard implant surface employed by clinicians today. If this standard implant surface group were utilized, it may have resulted in decreased reduction in *P. gingivalis* attachment onto the silver and non-silver nanotubular surface compared to the standard implant surface group, as the current data collected suggested that surface chemistry, surface roughness, surface wettability, and surface free energy may be the main promoters of biological cell attachment onto titanium surfaces. The reduction of bacterial attachment on the silver nanotubular surface may still be significant compared to a standard roughness titanium implant surface. The biocompatibility of the novel surfaces may also be the same compared to the real-world clinical control surface.

The small sample size of the study (10 surfaces per group for bacterial attachment per experiment) also greatly weakened the power of the study. The study was mainly a proof of concept of the potential antimicrobial properties of the novel titania nanotubular surface. *In vitro* dental implants experience more dynamic handling and complex environment, and these are factors (i.e. physical surface stability and various extracelluluar proteins) that can provide more useful insight on the clinical application of the surface. Also, the study was short term and did not look at how long-term aging and how the intraoral environment could affect the surface behavior.

The weakest surface characterization test was likely the white light interferometry. The analysis captured a picture of the surface and gave an average surface roughness value, and this study had three sites sampled per surface group. Perhaps upwards of 10 sites per 10 samples per group would provide more power and validity to the results.

For good, reliable results, the standard FESEM analysis should have at least 10 random, separate sites viewed under the microscope.[72] For our study, only 2 sites were viewed per sample, and there were two samples per group per experiment. The crystal violet stain that was used for the *in vitro* attachment assay worked mainly on the lipopolysaccharide membrane of Gram-positive bacteria. Perhaps other kinds of standard bacterial attachment assay, such as confocal microscopy, and XTT assay, could be used in future experiments to confirm or deny the results.

Due to the limitations of this study, the authors were not able to assess if the increased time of silver deposition, during the reverse polarization part of the anodization protocol, actually resulted in increased silver content of the nanotubular surface. We could confirm that all of the silver embedded surface groups have silver from the EDX spectra. Ultimately, all of the results for the silver experimental groups appear to be the same. It may also be that the primary effect was the result of residual electrolyte on all of the surfaces resulting in the same early outcomes measured. It is also possible that other mechanisms may be at play. Further studies such as silver release and sectional TEM images can confirm the amount of silver in the nanotubular surface and the potential release of the silver over time, which may affect and modulate the host cellular response and esthetic epithelial tissue outcomes. Furthermore, if silver did indeed have an effect and was being released, future studies on ways to control the silver release are recommended. Potential ways to initiate or halt the silver release may by using an UV light intraorally or a pH rinse to activate or deactivate the surface. The potential to have a surface characteristic

that can be controlled at different times would be helpful for more controlled applications, as in the case of natural intraoral disease progression.

The results of the silver experimental groups were a function of both the change in the surface topography as well as the presence of silver. The nanotubes surface treatment in general rendered the surface more hydrophilic with greater surface roughness compared to CP-Ti, and the incorporation of silver seemed to decrease hydrophilicity and surface roughness compared to nonsilver nanotubular surface. The data did not show if there were any differences among the silver groups and the exact influence of additional silver deposition. More material and surface characterization and behavior studies are recommended for future studies to better clarify the influence of silver in the nanotubes.

5.6 Clinical Relevance

Based on the literature review, silver has shown to be an effective antimicrobial agent for not only *P. gingivalis*, but also other bacteria that are initial colonizers.[72] Beyond future recommended tests described later to continue better understanding of the fabricated novel dental implant surface, silver can be investigated in other types of dental surfaces for their antimicrobial properties. The titanium nanotubular surface alone had desirable surface wettability and roughness, and current commercial dental implant surfaces can be modified and tested to include titanium nanotubes on the surface for potentially better bone response (decreased osseointegration time in the short term and better marginal bone level maintenance in the long term) and higher clinical dental implant success.

A dental implant has various potential interfaces: osseous, transepithelial, and intraoral (cavity). Each interface requires different needs from the implant surface. The osseous interface requires a hydrophilic, rough, and biocompatible surface for osseointegration with osteoblastic cells. The transepithelial interface requires a smooth, biocompatible, and potentially antimicrobial surface for epithelial attachment, decreased bioflilm formation, and decreased inflammation. The oral cavity interface requires a mechanically strong and smooth surface for proper reciprocation and function with prosthetic components. The ideal implant should provide the optimal surface environment for all of the interfaces. The novel dental implant surface we have created deals primarily with the coronal aspect of the osseous interface as well as the transepithelial surface to help control for soft tissue response and ongoing health. Ideally, the surface should

promote some osseous and soft tissue attachment via surface morphology and surface roughness, much like BioLok Biohorizon system that has documented *in vitro* and short term clinical success.[97, 98] Biolok has laser microtexturing of the surface and seemed to facilitate biologic width better than machined surfaces. The epithelial cells seemed to proliferate well on the textured surface.

The goal of this and many other dental implant surface study is to create an implant surface with improved ongoing hard and soft tissue health while reducing inflammation via reduced bacterial attachment on the surface.

6 CONCLUSIONS

6.1 Summary

The results of this research project allowed the authors to accept hypothesis #1-3, but further research is necessary to determine if hypothesis #4 can be accepted.

The first aim of this study was to fabricate silver deposited and non-silver deposited titania nanotubes using electrochemical anodization technique. A literature review of surface modifications for titanium dental implants led the authors to postulate that a titanium nanotubular surface embedded with silver could be fabricated and would have dynamic and desirable characteristics for osseointegration, bone maintenance, and bacterial resistance in the face of peri-implant conditions. After preliminary studies and characterizations of the surface, the silver deposited and non-silver deposited titania nanotubular surfaces were successfully fabricated using electrochemical anodization technique to desired nanotubular dimensions. Based on surface characterization methods of water contact angle analysis, FTIR, EDS, and FESEM, the surfaces were observed to be stable, uniform, and uncontaminated with well-organized nanotubes. The surfaces were plated with *P. gingivalis* to determine the bacterial attachment. After 12 hours of incubation of both inoculated and sterile surfaces, *in vitro* assay via crystal violet staining and live/dead stain analysis were performed to observe the bacterial attachment. The silver embedded nanotubular surfaces had significant reduction (>83%) of bacterial attachment compared to the commercially pure titanium and titanium nanotubular surface without silver. These results allowed the authors to accept hypothesis #1-3.

The fourth aim of this study was to optimize an effective *in vitro* silver concentration for *P. gingivalis* growth inhibition. After the first set of experiments, there was no significant difference in reduction of bacterial attachment among the 3 different types of silver embedded surfaces. Therefore, the authors decided to create another surface with considerably more silver to determine if bactericidal silver embedded nanotubular surface could be fabricated. Based on the results and errors inherent with the types of analysis and assays performed, the authors could not determine if the silver embedded nanotubular surface was bactericidal. Further research and different kinds of testing would be necessary to determine if this surface was bactericidal. At this time, the authors could not accept hypothesis #4.

The results of this research study allowed the authors to make the following conclusions:

1. Silver-embedded and non-silver-embedded titania nanotubular surfaces were successfully fabricated on a commercially pure titanium surface
2. Titanium nanotubular surfaces have increased surface wettability and surface roughness compared to commercially pure titanium surfaces.
3. The incorporation of silver into titanium nanotubular surface decreased hydrophilicity of the surface compared to titania nanotubular surface with no silver, but the silver also decreased the surface roughness to a more commercially accepted R_a value.
4. The silver embedded titania nanotubular surface has more favorable surface characteristics than commercially pure titanium surface.

5. The water contact angles of TiNT and TiNT-Ag were stable over 26 days.
6. Silver-embedded titania nanotubular surfaces suppressed the attachment of *P. gingivalis* biofilm compared to titania nanotubular surfaces with no silver.
7. The antimicrobial properties of TiNT-Ag surfaces may reduce bacterial colonization and associated peri-implantitis.

6.2 Recommendations for Future Work

Silver release and sequelae: The protocols that were followed and performed were not able to determine the exact amount of silver that may have been released from the nanotubular surfaces over time, although previous studies exist to prove that silver was stable in titanium nanotubes and would not leach out into the surrounding environment.[76] This information would be useful and provide a more comprehensive analysis of the surface and its potential in clinical applications. In the scenario that the silver was released from the surface, there would be concerns of biocompatibility, adjacent tissue discoloration, and potential adjacent restorative material discoloration, as seen in greening of porcelain in full coverage dental crown restorations with both silver and porcelain.[74,99] However some studies showed that the corrosion and tarnishing abilities of different elements in different metal alloys was related to amount and relative proportion of the elements in an alloy.[75] Perhaps the relatively high proportion of titanium in the novel nanotubular surface fabricated in this study could provide corrosion resistance for both the titanium and silver on the nanotubular surface.

***In Vitro* Bacterial Attachment Assay:** Other ways to assess bacterial attachment would be confocal microscopy and agar plating. These methods may provide a more visual assessment of bacterial attachment and growth inhibition than crystal violet stain. Similar protocol could also be conducted with different bacteria. For example, *Streptococcus mutans* in the supragingival plaque and *Prevotella intermedia* of subgingival calculus are both good targets of antimicrobial assessment of dental prosthetic surfaces. A combination of both an initial and late colonizer of the known human intraoral plaque could be plated

together to simulate natural biofilms and observe any symbiotic behavior between the two bacteria for increased bacterial attachment.

Biocompatibility of surface: Test for cytotoxicity and tissue irritation MG-63 cell line is a human osteosarcoma cell line that is biologically different from human osteoblasts, and MG-63 is used in research for osteoblast models.[100] The extracellular matrix contents of cell line are different from that of osteoblast cells. The gene expression of various osteoblast cell growth proteins could be analyzed to observe the direction of cell cultural growth for biocompatibility testing. If TiNT-Ag surfaces were found to be unbiocompatible, then other drugs, such as vancomycin, and elements could be considered for antimicrobial additions to TiNT surfaces.[101]

Materials Properties, Characterization, and Behavior and *in vivo* testing: Only certain surface qualities of the novel titania nanotubular surface with and without silver were investigated. After going through the previously recommended studies and if the surface continues to present desirable results, then the surface can be synthesized and tested for other mechanical properties and characteristics (hardness, nano-indentation, friction, wear, etc). The nanotubular surface could also be altered in layers for improved behaviors.[102] The surfaces can also be tested *in vivo.* For example, analog dental implants could be implanted into rat or pig femurs or mandibles. Multiple assessments could then be made from the test such as histologic osseointegration evaluation, implant success rates, other soft tissue response, potential allergenicity, surface stability and integrity post testing, etc. The response of epithelial cells to the surface would provide pertinent host

response and potential esthetic influence information. Such tests would provide pertinent information on implant treatment and thus, are highly recommended before human testing in randomized clinical trials.

7 CITED LITERATURE

1. Salinas TJ, Block MS, Sadan A. Fixed partial denture or single-tooth implant restoration? Statistical considerations for sequencing and treatment. J Oral Maxillofac Surg 2004;62(9 Suppl 2):2-16.
2. Jung RE, Pjetursson BE, Glauser R, *et al.* . . A systematic review of the 5-year survival and complication rates of implant-supported single crowns. Clin Oral Implants Res 2008;19(2):119-30.
3. Moraschini V, Velloso G, Luz D, Porto Barboza E. Implant survival rates, marginal bone level changes, and complications in full-mouth rehabilitation with flapless computer-guided surgery: a systematic review and meta-analysis. Int J Oral Maxillofac Surg 2015.
4. Albrektsson T, Zarb G, Worthington P, Eriksson AR. The long-term efficacy of currently used dental implants: a review and proposed criteria of success. Int J Oral Maxillofac Implants 1986;1(1):11-25.
5. Papaspyridakos P, Chen CJ, Chuang SK, Weber HP, Gallucci GO. A systematic review of biologic and technical complications with fixed implant rehabilitations for edentulous patients. Int J Oral Maxillofac Implants 2012;27(1):102-10.
6. Gao Y, Li Y, Xiao J, *et al.* . . Effects of microrough and hierarchical hybrid micro/nanorough surface implants on osseointegration in ovariectomized rats: A longitudinal in vivo microcomputed tomography evaluation. J Biomed Mater Res A 2012;100(8):2159-67.
7. Qian J WA, Albrektsson T. Reasons for Marginal Bone Loss around Oral Implants. Clinical Implant Dentistry and Related Research 2012;14(6):792-807.
8. Esposito M, Grusovin MG, Worthington HV. Treatment of peri-implantitis: what interventions are effective? A Cochrane systematic review. Eur J Oral Implantol 2012;5 Suppl:S21-41.
9. Banche G, Roana J, Mandras N, *et al.* . . Microbial adherence on various intraoral suture materials in patients undergoing dental surgery. J Oral Maxillofac Surg 2007;65(8):1503-7.
10. Zhao L, Wang H, Huo K, *et al.* . . Antibacterial nano-structured titania coating incorporated with silver nanoparticles. Biomaterials 2011;32(24):5706-16.
11. Darouiche RO. Treatment of infections associated with surgical implants. N Engl J Med 2004;350(14):1422-9.
12. Zhao L, Chu PK, Zhang Y, Wu Z. Antibacterial coatings on titanium implants. J Biomed Mater Res B Appl Biomater 2009;91(1):470-80.
13. Branemark PI, Hansson BO, Adell R, *et al.* . . Osseointegrated implants in the treatment of the edentulous jaw. Experience from a 10-year period. Scand J Plast Reconstr Surg Suppl 1977;16:1-132.
14. Albrektsson T, Branemark PI, Hansson HA, Lindstrom J. Osseointegrated titanium implants. Requirements for ensuring a long-lasting, direct bone-to-implant anchorage in man. Acta Orthop Scand 1981;52(2):155-70.
15. Prosthodontics TAo. Glossary of Prosthodontics Terms, 8th Edition. Journal of Prosthetic Dentistry July 2005;94(1):10-92.
16. Albrektsson T, Jacobsson M. Bone-metal interface in osseointegration. J Prosthet Dent 1987;57(5):597-607.

17. Albrektsson T, Johansson C. Osteoinduction, osteoconduction and osseointegration. Eur Spine J 2001;10 Suppl 2:S96-101.
18. Davies JE. Understanding peri-implant endosseous healing. J Dent Educ 2003;67(8):932-49.
19. Morris HF, Ochi S. Hydroxyapatite-coated implants: a case for their use. J Oral Maxillofac Surg 1998;56(11):1303-11.
20. Gredes T, Kubasiewicz-Ross P, Gedrange T, Dominiak M, Kunert-Keil C. Comparison of surface modified zirconia implants with commercially available zirconium and titanium implants: a histological study in pigs. Implant Dent 2014;23(4):502-7.
21. O'Brien WJ. Dental Materials and Their Selection; 4th Edition 4th Edition ed: Quintessence Pub Co; 2009.
22. Velten D, Biehl V, Aubertin F, *et al.* . . Preparation of TiO(2) layers on cp-Ti and Ti6Al4V by thermal and anodic oxidation and by sol-gel coating techniques and their characterization. J Biomed Mater Res 2002;59(1):18-28.
23. Neumann A.W. GRJ. Thermodynamics of contact angles I. Heterogenous Solid Surfaces. Journal of Colloid and Interface Science 1972;38(2):341-58.
24. Giljean S. BM, Anselme K., Haidara H. . New insights on contact angle/roughness dependence on high surface energy materials. Applied Surface Science 2011;257(22):9631-38.
25. Oliver J F HC, Mason S G The Apparent Contact Angle of Liquids of Finely-Grooved Solid Surfaces - A SEM Study Journal of Adhesion 1976;8(3):223-34.
26. Mekayarajjananonth T, Winkler S. Contact angle measurement on dental implant biomaterials. J Oral Implantol 1999;25(4):230-6.
27. Albrektsson T, Wennerberg A. Oral implant surfaces: Part 1--review focusing on topographic and chemical properties of different surfaces and in vivo responses to them. Int J Prosthodont 2004;17(5):536-43.
28. Jokstad A, Braegger U, Brunski JB, *et al.* . . Quality of dental implants. Int Dent J 2003;53(6 Suppl 2):409-43.
29. Xuereb M, Camilleri J, Attard NJ. Systematic review of current dental implant coating materials and novel coating techniques. Int J Prosthodont 2015;28(1):51-9.
30. Liu R, Lei T, Dusevich V, *et al.* . . Surface characteristics and cell adhesion: a comparative study of four commercial dental implants. J Prosthodont 2013;22(8):641-51.
31. Prato M, Kostarelos K, Bianco A. Functionalized carbon nanotubes in drug design and discovery. Acc Chem Res 2008;41(1):60-8.
32. Kam NW, Liu Z, Dai H. Functionalization of carbon nanotubes via cleavable disulfide bonds for efficient intracellular delivery of siRNA and potent gene silencing. J Am Chem Soc 2005;127(36):12492-3.
33. Feazell RP, Nakayama-Ratchford N, Dai H, Lippard SJ. Soluble single-walled carbon nanotubes as longboat delivery systems for platinum(IV) anticancer drug design. J Am Chem Soc 2007;129(27):8438-9.
34. Liu Z, Chen K, Davis C, *et al.* . . Drug delivery with carbon nanotubes for in vivo cancer treatment. Cancer Res 2008;68(16):6652-60.
35. Chen J, Chen S, Zhao X, *et al.* . . Functionalized single-walled carbon nanotubes as rationally designed vehicles for tumor-targeted drug delivery. J Am Chem Soc 2008;130(49):16778-85.

36. Rajyalakshmi A, Ercan B, Balasubramanian K, Webster TJ. Reduced adhesion of macrophages on anodized titanium with select nanotube surface features. Int J Nanomedicine 2011;6:1765-71.
37. Sun X, Liu Z, Welsher K, *et al.* . . Nano-Graphene Oxide for Cellular Imaging and Drug Delivery. Nano Res 2008;1(3):203-12.
38. Liu Z, Sun X, Nakayama-Ratchford N, Dai H. Supramolecular chemistry on water-soluble carbon nanotubes for drug loading and delivery. ACS Nano 2007;1(1):50-6.
39. Hu Y, Cai K, Luo Z, *et al.* . . TiO2 nanotubes as drug nanoreservoirs for the regulation of mobility and differentiation of mesenchymal stem cells. Acta Biomater 2012;8(1):439-48.
40. Monteiro DR, Gorup LF, Takamiya AS, *et al.* . . The growing importance of materials that prevent microbial adhesion: antimicrobial effect of medical devices containing silver. Int J Antimicrob Agents 2009;34(2):103-10.
41. Abdi Y, Barati F. Variable electron beam diameter achieved by a titanium oxide/carbon nanotube hetero-structure suitable for nanolithography. Nanotechnology 2013;24(5):055303.
42. Patole SP, Shin DW, Fugetsu B, Yoo JB. Filtration-wet transferred transparent conducting films of mm long carbon nanotubes grown using water-assisted chemical vapor deposition. J Nanosci Nanotechnol 2013;13(11):7413-7.
43. Hamlekhan A, Butt A, Patel S, Royhman D, Takoudis C, et al. (2014) Fabrication of Anti-Aging TiO_2 Nanotubes on Biomedical Ti Alloys. PLoS ONE 9(5):e96213. doi: 10.1371/journal.pone.0096213
44. Singh AV, Vyas V, Patil R, *et al.* . . Quantitative characterization of the influence of the nanoscale morphology of nanostructured surfaces on bacterial adhesion and biofilm formation. PLoS One 2011;6(9):e25029.
45. RN W. Surface roughness and contact angle. J Phys Colloid Chem 1949;53:1466-67.
46. Frojd V, Linderback P, Wennerberg A, *et al.* . . Effect of nanoporous TiO2 coating and anodized Ca2+ modification of titanium surfaces on early microbial biofilm formation. BMC Oral Health 2011;11:8.
47. Ercan B, Taylor E, Alpaslan E, Webster TJ. Diameter of titanium nanotubes influences anti-bacterial efficacy. Nanotechnology 2011;22(29):295102.
48. Zhao L, Mei S, Chu PK, Zhang Y, Wu Z. The influence of hierarchical hybrid micro/nano-textured titanium surface with titania nanotubes on osteoblast functions. Biomaterials 2010;31(19):5072-82.
49. Duncan WJ, Lee MH, Dovban AS, *et al.* . . Anodization increases early integration of Osstem implants in sheep femurs. Ann R Australas Coll Dent Surg 2008;19:152-6.
50. Brammer KS, Frandsen CJ, Jin S. TiO2 nanotubes for bone regeneration. Trends Biotechnol 2012;30(6):315-22.
51. Oh S, Brammer KS, Li YS, *et al.* . . Stem cell fate dictated solely by altered nanotube dimension. Proc Natl Acad Sci U S A 2009;106(7):2130-5.
52. Park J, Bauer S, von der Mark K, Schmuki P. Nanosize and vitality: TiO2 nanotube diameter directs cell fate. Nano Lett 2007;7(6):1686-91.
53. Shokuhfar T, Hamlekhan A, Chang JY, *et al.* . . Biophysical evaluation of cells on nanotubular surfaces: the effects of atomic ordering and chemistry. Int J Nanomedicine 2014;9:3737-48.

54. Mouhyi J, Dohan Ehrenfest DM, Albrektsson T. The peri-implantitis: implant surfaces, microstructure, and physicochemical aspects. Clin Implant Dent Relat Res 2012;14(2):170-83.
55. Lindhe J, Meyle J, Group DoEWoP. Peri-implant diseases: Consensus Report of the Sixth European Workshop on Periodontology. J Clin Periodontol 2008;35(8 Suppl):282-5.
56. Heitz-Mayfield LJ. Peri-implant diseases: diagnosis and risk indicators. J Clin Periodontol 2008;35(8 Suppl):292-304.
57. Derks J. TC. Peri-implant health and disease. A systematic review of current epidemiology. Journal of Clinical Periodontology 2015;42(S16):S158-S71.
58. Gristina AG. Biomaterial-centered infection: microbial adhesion versus tissue integration. Science 1987;237(4822):1588-95.
59. Ata-Ali J, Candel-Marti ME, Flichy-Fernandez AJ, *et al.* . . Peri-implantitis: associated microbiota and treatment. Med Oral Patol Oral Cir Bucal 2011;16(7):e937-43.
60. Xing Z, Pabst MJ, Hasty KA, Smith RA. Accumulation of LPS by polyethylene particles decreases bone attachment to implants. J Orthop Res 2006;24(5):959-66.
61. Teughels W, Van Assche N, Sliepen I, Quirynen M. Effect of material characteristics and/or surface topography on biofilm development. Clin Oral Implants Res 2006;17 Suppl 2:68-81.
62. Park JE, Barbul A. Understanding the role of immune regulation in wound healing. Am J Surg 2004;187(5A):11S-16S.
63. Zheng Y, Li J, Liu X, Sun J. Antimicrobial and osteogenic effect of Ag-implanted titanium with a nanostructured surface. Int J Nanomedicine 2012;7:875-84.
64. Green SA, Ripley MJ. Chronic osteomyelitis in pin tracks. J Bone Joint Surg Am 1984;66(7):1092-8.
65. Gil FJ, Rodriguez A, Espinar E, *et al.* . . Effect of oral bacteria on the mechanical behavior of titanium dental implants. Int J Oral Maxillofac Implants 2012;27(1):64-8.
66. Newman M G TH, Carranza F A, Klokkevold P R. Carranza's Clinical Periodontology. 10 ed: Saunders; 2006.
67. Yoshimura F, Murakami Y, Nishikawa K, Hasegawa Y, Kawaminami S. Surface components of Porphyromonas gingivalis. J Periodontal Res 2009;44(1):1-12.
68. Yilmaz O. The chronicles of Porphyromonas gingivalis: the microbium, the human oral epithelium and their interplay. Microbiology 2008;154(Pt 10):2897-903.
69. Sheets SM, Robles-Price AG, McKenzie RM, Casiano CA, Fletcher HM. Gingipain-dependent interactions with the host are important for survival of Porphyromonas gingivalis. Front Biosci 2008;13:3215-38.
70. Takanashi K, Kishi M, Okuda K, Ishihara K. Colonization by Porphyromonas gingivalis and Prevotella intermedia from teeth to osseointegrated implant regions. Bull Tokyo Dent Coll 2004;45(2):77-85.
71. Kim ML, Jeong CM, Jeon YC, *et al.* . . The effects of Mg-ion implantation and sandblasting on Porphyromonas gingivalis attachment. Clin Oral Implants Res 2012;23(2):245-52.
72. Wu-Yuan CD, Eganhouse KJ, Keller JC, Walters KS. Oral bacterial attachment to titanium surfaces: a scanning electron microscopy study. J Oral Implantol 1995;21(3):207-13.

73. Barao VA, Yoon CJ, Mathew MT, *et al.* . . Attachment of Porphyromonas gingivalis to corroded commercially pure titanium and titanium-aluminum-vanadium alloy. J Periodontol 2014;85(9):1275-82.
74. Powers J M SRL. Craig's Restorative Dental Materials, 12E. 12 ed: Mosby; 2006.
75. Lang B R BSH, Giday Z, Asgar K. Tarnish and Corrosion of Noble Metal Alloys. The Journal of Prosthetic Dentistry 1982;48(3):245-52.
76. Alt V, Bechert T, Steinrucke P, *et al.* . . An in vitro assessment of the antibacterial properties and cytotoxicity of nanoparticulate silver bone cement. Biomaterials 2004;25(18):4383-91.
77. Juan L, Zhimin Z, Anchun M, Lei L, Jingchao Z. Deposition of silver nanoparticles on titanium surface for antibacterial effect. Int J Nanomedicine 2010;5:261-7.
78. Vargas-Reus MA, Memarzadeh K, Huang J, Ren GG, Allaker RP. Antimicrobial activity of nanoparticulate metal oxides against peri-implantitis pathogens. Int J Antimicrob Agents 2012;40(2):135-9.
79. Darouiche RO. Anti-infective efficacy of silver-coated medical prostheses. Clin Infect Dis 1999;29(6):1371-7; quiz 78.
80. Song H Y KKK, Oh I. H, Lee B. T. . Fabrication of Silver Nanoparticles and Their Antimicrobial Mechanisms. European Cells and Materials 2006;11(1):58.
81. Morones JR, Elechiguerra JL, Camacho A, *et al.* . . The bactericidal effect of silver nanoparticles. Nanotechnology 2005;16(10):2346-53.
82. De Matteis V, Malvindi MA, Galeone A, *et al.* . . Negligible particle-specific toxicity mechanism of silver nanoparticles: The role of Ag(+) ion release in the cytosol. Nanomedicine 2015;11(3):731-9.
83. A. S. Au, S. Patel, W. Li, C. D. Wu, T. Shokuhfar, C. Sukotjo. March 2015 Silver-embedded titania nanotubes surfaces inhibit attachment of *Porphyromonas gingivalis* biofilm. Abstract presented at the annual session of International Association of Dental Research Conference in Boston, Massachusetts, USA.
84. Papaioannou W, van Steenberghe D, Cassiman JJ, Van Eldere J, Quirynen M. Comparison of fluorescence microscopy and culture assays to quantitate adhesion of Porphyromonas gingivalis to mono- and multi-layered pocket epithelium cultures. J Periodontol 1999;70(6):618-25.
85. Bezrodna, T., et al., *IR-analysis of H-bonded H2O on the pure TiO2 surface.* Journal of Molecular Structure, 2004. **700**(1–3): p. 175-181.
86. Zeitler, V.A. and C.A. Brown, *The Infrared Spectra of Some Ti-O-Si, Ti-O-Ti and Si-O-Si Compounds.* The Journal of Physical Chemistry, 1957. **61**(9): p. 1174-1177.
87. Wu, R.-J., et al., *Composite of TiO2 nanowires and Nafion as humidity sensor material.* Sensors and Actuators B: Chemical, 2006. **115**(1): p. 198-204.
88. Liang, Y.Q., et al., *Silver nanoparticles supported on TiO2 nanotubes as active catalysts for ethanol oxidation.* Journal of Catalysis, 2011. **278**(2): p. 276-287.
89. Sheibley, D.W. and M.H. Fowler, *Infrared spectra of various metal oxides in the region of 2 to 26 microns. NASA TN D-3750.* Tech Note U S Natl Aeronaut Space Adm, 1967: p. 1-62.
90. Fahim, N.F. and T. Sekino, *A Novel Method for Synthesis of Titania Nanotube Powders using Rapid Breakdown Anodization.* Chemistry of Materials, 2009. **21**(9): p. 1967-1979.

91. Cesano, F., et al., *Designing TiO2 Based Nanostructures by Control of Surface Morphology of Pure and Silver Loaded Titanate Nanotubes.* The Journal of Physical Chemistry C, 2010. **114**(1): p. 169-178.
92. Bezrodna, T., et al., *Spectroscopic study of TiO2 (rutile)–benzophenone heterogeneous systems.* Journal of Molecular Structure, 2002. **614**(1–3): p. 315-324.
93. Fujishima, A., X. Zhang, and D.A. Tryk, *TiO2 photocatalysis and related surface phenomena.* Surface Science Reports, 2008. **63**(12): p. 515-582.
94. Joshi, K.M. and V.S. Shrivastava, *Photocatalytic degradation of Chromium (VI) from wastewater using nanomaterials like TiO2, ZnO, and CdS.* Applied Nanoscience, 2011. **1**(3): p. 147-155.
95. Dhonge, B.P., et al., *Spray pyrolytic deposition of transparent aluminum oxide (Al2O3) films.* Applied Surface Science, 2011. **258**(3): p. 1091-1096.
96. Freund, H.J. and M.W. Roberts, *Surface chemistry of carbon dioxide.* Surface Science Reports, 1996. **25**(8): p. 225-273.
97. Taylor RC[1], McGlumphy EA, Tatakis DN, Beck FM. Radiographic and clinical evaluation of single-tooth Biolok implants: a 5-year study. Int J Oral Maxillofac Implants. 2004 Nov-Dec;19(6):849-54.
98. Weiner S[1], Simon J, Ehrenberg DS, Zweig B, Ricci JL. The effects of laser microtextured collars upon crestal bone levels of dental implants. Implant Dent. 2008 Jun;17(2):217-28.
99. Joska L, Venclikova Z, Poddana M, Benada O. The mechanism of gingiva metallic pigmentations formation. Clin Oral Investig 2009;13(1):1-7.
100. Zhang D, Ren L, Zhang Y, *et al.* . . Antibacterial activity against Porphyromonas gingivalis and biological characteristics of antibacterial stainless steel. Colloids Surf B Biointerfaces 2013;105:51-7.
101. Ordikhani F, Tamjid E, Simchi A. Characterization and antibacterial performance of electrodeposited chitosan-vancomycin composite coatings for prevention of implant-associated infections. Mater Sci Eng C Mater Biol Appl 2014;41:240-8.
102. Kazemzadeh-Narbat M, Lai BF, Ding C, *et al.* . . Multilayered coating on titanium for controlled release of antimicrobial peptides for the prevention of implant-associated infections. Biomaterials 2013;34(24):5969-77.
103. Patel S, Hamlekan A, Royhman D, Butt A, Yuan J, Shokuhfar T, Sukotjo C, Matthew MT, Jurisch G, Takoudis CG. Enhancing surface characteristics of Ti–6Al–4V for bio-implants using integrated anodization and thermal oxidation. *J. Mater. Chem. B*, 2014,2, 3597-3608
104. FY 2014-2015 Annual Report. (2015 July). Retrieved from http://www.mtu.edu/research/about/centers-institutes/docs/MuSTI-annual-report.pdf

8 APPENDIX

8.1 VITA

Amy S. Au

801 South Paulina, R361, Chicago, Illinois 60612

Cell (510) 709-7181 :: amysau@gmail.com

Curriculum Vitae

Summary of Qualifications:

- ✓ Doctor of Dental Surgery program graduate from University of the Pacific, 2012
- ✓ Certificate in Advanced Prosthodontics Program from UIC, 2015
- ✓ Competent in Prosthodontics and Restorative dentistry –literature and clinical
- ✓ Qualified in de not ntal implant surgical placement and restorations
- ✓ Invisalign Certified - capable of case completion
- ✓ Basic Life Support & CPR certified– exp. 06/04/2016

Education:

2012 – 2015 University of Illinois at Chicago College of Dentistry, Chicago, IL
- ➢ Certificate in Advanced Prosthodontics
- ➢ Masters of Oral Science Candidate; Anticipated December 2015

2009 – 2012 University of the Pacific Arthur A. Dugoni School of Dentistry, San Francisco, CA
- ➢ Doctor of Dental Surgery

2007 – 2009 University of the Pacific, Stockton, CA
- ➢ Bachelor of Arts in Applied Science

Dental Licensure:

2012 – present	California	Active
2012 – present	Illinois	Active

Boards Certification:

National Dental Boards Examination Part I & II	Pass 2011 and 2012
Western Regional Examination Boards	Pass May 2012
American Boards of Prosthodontics	Pass A, B II & IV, Anticipated B III 2/2015

Academic Appointments:

07/2015-present University of the Pacific Arthur A. Dugoni School of Dentistry, San Francisco, CA
- ➢ Clinical Assistant Professor

05/2015-12/2015 University of Illinois at Chicago College of Dentistry, Chicago, IL
- ➢ Clinical Assistant Professor

Professional Experience & Externships:

06/13/11 – 06/22/11 University of Michigan, School of Dentistry, Postgraduate Prosthodontics Clinic, Ann Arbor, MI
- ➢ Observed and assisted removable, fixed, and implant prosthodontic procedures and surgery

6/2011 University of Maryland School of Dentistry, Baltimore, MD

6/2011 University of Connecticut, School of Dental Medicine, Farmington, CT

03/21/11 – 03/25/11 Community Medical Center, Level I Trauma Clinic, Fresno, CA

- Observed and assisted mandibular fractures, free flap, reanastomoses, and facial prosthetic implant reconstruction surgeries in the OR and standard OMFS clinic procedures

2010-2011 University of the Pacific Arthur A. Dugoni School of Dentistry, SF, CA

- Student Dental Anatomy, Anatomy, and Biochemistry Tutor

06/14/10 – 06/25/10 Indian Health Services, White Earth Health Center, White Earth, MN

- Observed and assisted simple restorative and extraction procedures

Extracurriculars:

2012 – 2015 University of Illinois at Chicago, College of Dentistry, Chicago, IL
Prosthodontic Implant Club: discuss current implant treatment plans and restorations

2010 – 2012 University of the Pacific Arthur A. Dugoni School of Dentistry, SF, CA
Student Leader: Clinic Ambassador for DDS Class of 2012

2010 – 2011 University of the Pacific Arthur A. Dugoni School of Dentistry, SF, CA
Student Ambassador

2010 – 2012 University of the Pacific Arthur A. Dugoni School of Dentistry, SF, CA
Club SCOPE: Participated in dental screenings and community outreach programs on oral health

2009 – 2010 University of the Pacific Arthur A. Dugoni School of Dentistry, SF, CA
Esthetics Study Club: seminar series by guest lecturers on esthetic dentistry

Research Activities and Grant Support:

2012 - 2015 "Silver Embedded titania nanotube surfaces inhibit attachment of *Porphyromonas gingivalis* biofilm. " Chief investigator
International Association of Dental Research Prosthodontics Group Student R. Fellowship $4500
Academy of Prosthodontics Student Grant $3750
American College of Prosthodontists Education Foundation Student Research Fellowship $6000
Greater New York Academy of Prosthodontists Student Grant $2000

2010 - 2012 "HIV Gene Therapy." Co-investigator

Publications:

- Gebremedhin S[1], Au A, Konopka K, Milnes M, Düzgüneş N. *A gene therapy approach to eliminate HIV-1-infected cells*.J Calif Dent Assoc. 2012 May;40(5):402-6.

Honors & Awards:

10/2015 American College of Prosthodontists, John S. Sharry Research Competition

- 2nd Place Winner

06/2012	Tau Kappa Omega, College of Physicians and Surgeons, Honors Society
06/2012	OKU Clinical Excellence Award in Removable Prosthodontics
06/2012	Quintessence Research Award – Outstanding Research Achievement
06/2012	Who's Who Among Students in American Colleges and Universities ➢ Outstanding Merit and Accomplishment
05/2011	Hinman Symposium Award, Excellence in Research
08/2007-05/2009	University of the Pacific – Dean's Honor Roll
08/2007-05/2009	University of the Pacific - Regent's Scholar
05/2009	Phi Beta Kappa, Academic Honors Society
05/2008	Alpha Lambda Delta National Honors Society

Professional Presentations:

10/2015	American College of Prosthodontists Annual Session, John S. Sharry Competition, 2nd Place Winner
03/2015	IADR Annual Session, Oral Presentation
11/2014	American College of Prosthodontists Annual Session, Poster Presentation Competition
09/2014 & 9/2013	UIC Annual Advanced Prosthodontics Program Clinical Presentations Day, Presentation
01/2014 & 1/2013	UIC Annual Advanced Prosthodontics Program Research Presentations Day, Presentation
03/2012	IADR Annual Session, Poster Presentation

Meetings & Professional Development:

- American College of Prosthodontists Annual Session (2012, 2013, 2014, 2015)
- American Academy of Fixed Prosthodontics, Annual Session (2012, 2013, 2014, 2015)
- American Prosthodontic Society, Annual Session (2012, 2013, 2014, 2015)
- Greater New York Academy of Prosthodontists Annual Session (2012 & 2013)
- International Association of Dental Research Annual Session (2012, 2013, 2015)
- Hinman Research Symposium (2011)

Professional/Scientific Organization Memberships:

➢ American College of Prosthodontists (ACP)	Member	2012 – present
➢ International Association of Dental Research (IADR)	Member	2012 – present
➢ American Dental Association (ADA)	Member	2009 – present
➢ California Dental Association (CDA)	Member	2009 – present
➢ American Student Dental Association (ASDA)	Member	2009 – present

Non-English Language:
Mandarin Chinese – Fluent, written and verbal

Hobbies & Interests:
Yoga, visual arts, musical & cultural appreciation, exploring new foods, making good memories with family & loved ones.

References Available Upon Request